Design, parameterization, and use of the Iowa State University UTR-10 for neutron radiography

by

Edmond George Wiegert

A Thesis Submitted to the
Graduate Faculty in Partial Fulfillment of the
Requirements for the Degree of
MASTER OF SCIENCE
Department: Mechanical Engineering
Major: Nuclear Engineering

Iowa State University
Ames, Iowa
1990

TABLE OF CONTENTS

LIST OF TABLES

LIST OF FIGURES

ABSTRACT

Neutron radiography has been used as a method of nondestructive examination which complements x-ray radiography. Neutron radiography differentiates materials by their nuclear properties while x-ray radiography differentiates materials by their electron densities.

The design of a facility to utilize neutrons leaking from the reactor through the west beamport of the Iowa State University UTR-10 Reactor for neutron radiography was detailed. The method used for recording an image of the object radiographed was the transfer method. This method involves activating an indium foil in proportion to the number of neutrons transmitted through the object radiographed; the activated foil then decays in proximity to an x-ray film "transferring" the image.

Methods to determine parameters were defined and measurements were made to determine the important parameters of the neutron beam: the neutron flux, the energy distribution, and degree of collimation. Parameters dealing with the radiographic method which were investigated were: the film unsharpness, the unsharpness due to transferring the image, and contributions to film density by the various radiations associated with the decay of indium-116m_1 isomer used to transfer the image. Neutron radiographs which exemplified the effects of the various parameters are included; as are possible methods to improve the images.

CHAPTER 1. INTRODUCTION

Uses of Neutron Radiography

Neutron radiography (NR) has developed at much the same pace as x-ray radiography. To illustrate this parallel development; the first x-ray radiographs were taken within a month of the discovery of x-rays by Roentgen [1] in 1895 while the first neutron radiographs were taken by Kallman and Kuhn [2] in the years from 1935 to 1938, several years after the discovery of the neutron in 1932 by Chadwick [3]. Both methods then had to wait about twenty years for necessary radiation sources to become reliable and intense enough to be used for routine applications [2,4,5,6]. When comparisons of the two processes are made, x-rays have had a distinct advantage over neutrons because of a forty-year headstart and a lower source cost. This is evidenced by the fact that x-rays were already included in specifications in boiler codes for shipping at the same time as the first neutron radiographs were taken.

Neutron radiography exploits the differing nuclear properties of each individual isotope that make up the object under investigation. The thermal neutron absorption and scattering cross-sections of materials, as given by a mass attenuation coefficient, can vary by more than four orders of magnitude; the equivalent x-ray linear absorption coefficient varies by only two orders of magnitude for 125 keV x-rays. The thermal neutron and x-ray attenuation coefficients are shown in Figure 1.1 as given by Harold [6] and others.

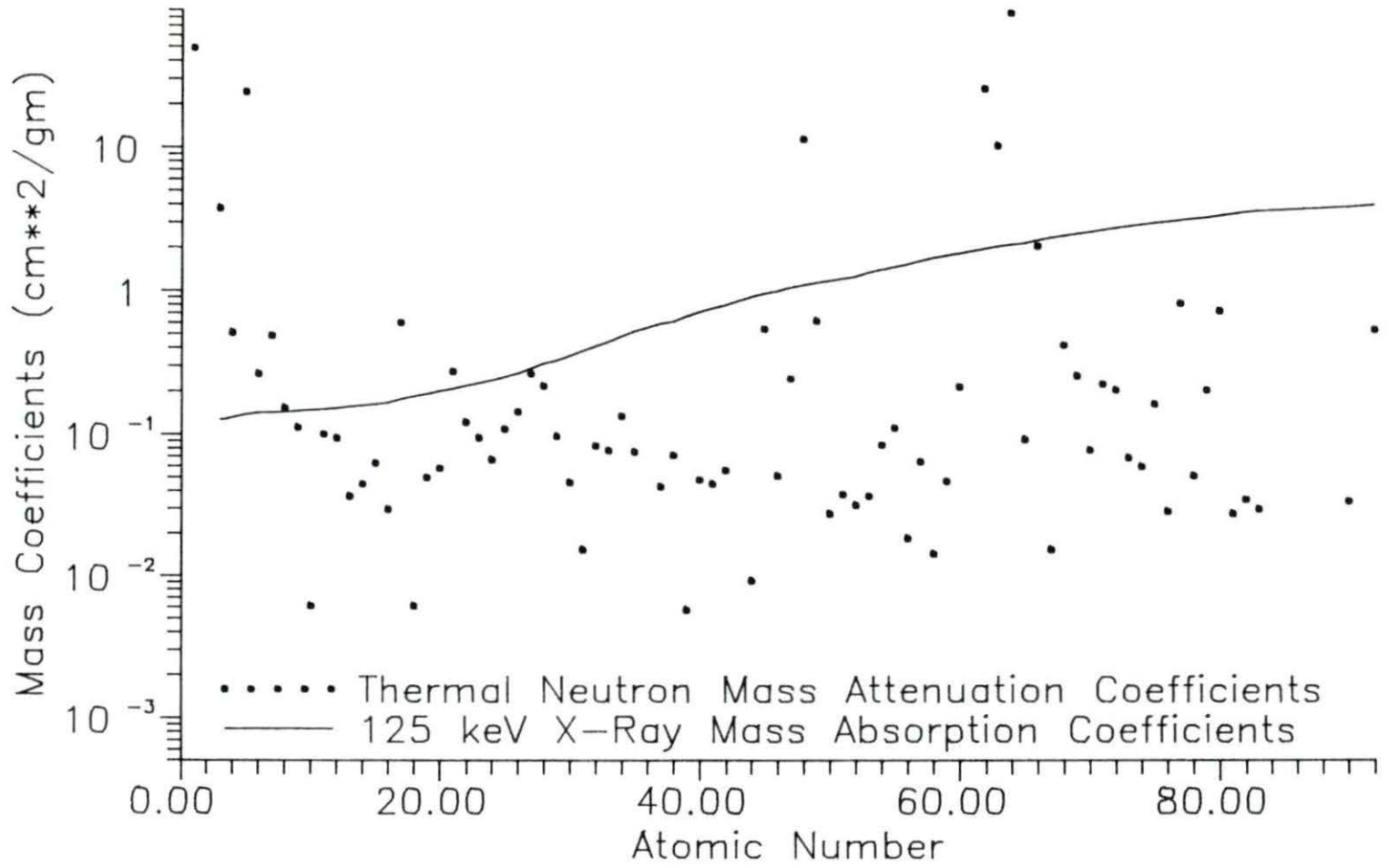

Figure 1.1: Mass Attenuation Coefficients of X- Rays and Thermal Neutrons for Comparing Properties Used For Radiographic Inspection

The large variations in the neutron scattering and absorption cross-sections should easily reflect the materials that comprise the object examined, as measured by the transmission of neutrons through the object. The portion of the neutrons transmitted through the object are then recorded as a two dimensional image on film which can then be used to infer information about the object. (More attenuation may indicate greater material thickness, or the inclusion of a material with different nuclear properties.)

Neutron and x-ray radiography are complementary inspection processes with similar techniques. Both use penetrating radiations which allow a relatively large thickness of material to be examined. They are both typically used to produce shadowgrams or pictures of the object under investigation. The interactions of neutrons and x-rays with matter are both energy dependent [1,2,3,4,5,6,7].

The difference between the two processes is in the aspects of the material to which neutrons and x-rays are sensitive. X-rays are affected by the electron density in the object under investigation. The number of electrons is directly related to the atomic number and the density of the material. Neutrons are affected by the scattering and absorption properties of the nuclei and their densities in the object under investigation. There is no relation between the nuclear properties and the atomic number or even the isotopes of the same element [1,2,3,4,5,6,7]. The large differences in neutronic properties between isotopes of the same or different elements makes NR a very sensitive nondestructive testing method in several areas of application.

Some examples of the use of NR are: 1) determining the isotopic constituents and abundances of an element for determining enrichment or depletion, 2) examining features in objects constructed of dense materials, 3) examining highly radioactive materials, and 4) detecting low Z materials that are surrounded by high Z materials.

Several investigations have been made which exploit the differences in neutron cross-sections

between isotopes of the same element to determine the burnup in boiling water reactor control rods [8,9] and the uranium enrichment in nuclear fuel rods [10,11,12]. Neutrons of energies other than thermal, which correspond to neutron absorption resonances, can be used to increase the detectability of the isotopes under investigation. Enrichment of nuclear fuel elements in materials like plutonium-239 has been determined by this method [13,14,15].

Neutron radiography has been used to investigate objects made of dense materials such as nuclear fuel elements. This is because x-rays do not readily penetrate materials like uranium, thorium, lead and bismuth [10,11,12].

Highly radioactive materials like nuclear fuel elements are inspected using NR [10,11,12]. This is because the high radiation field from the material exposes the x-ray film decreasing the possible contrast of the image.

The high interaction cross-section (mainly scattering) of hydrogen allows hydrogenous materials that are encased in metals to be examined. The electron density of the metal is usually much higher than in the hydrogenous material so the x-rays do not record the hydrogen bearing material. Since neutrons are much more sensitive to the hydrogen than most metals, the inner material is recorded instead of the metal. This application was used by NASA to inspect the explosive bolts used on the lunar landers, and the Army uses it to examine other explosives [16,17,18,19]. The high scattering cross-section of hydrogen allows it to be used as a marker when inspecting materials suspected of suffering from corrosion, since hydrogen is often a major component of corrosion byproduct materials [10,11,12,20,21,22,23,24,25].

Inspection of cast aircraft turbine blades is aided by tagging the casting material with a neutron absorbing material like gadolinium to determine whether all the casting material has been removed [26]. Gadolinium has also been used as a penetrant to highlight cracks in materials [17].

Scope

The major thrust of this investigation was to design and build a facility for NR from inexpensive materials, using the Iowa State University UTR-10 Research Reactor as the neutron source. After the construction of the facility was completed, the neutron beam and the process of recording the image were characterized using parameters affecting image quality. Many of these parameters are material dependent, so the characterizations which are material dependent will be centered on investigation of flaws in aluminum.

Finally, the feasibility of using NR to inspect for corrosion in aluminum as an example problem for the aircraft industry was examined, since NR is receiving serious attention for inspection of commercial aircraft and aluminum structures. The hydrogen which accompanies the corrosion can be detected by NR. Neutron radiography is currently used to inspect military aircraft [20,21,22,23,24,25,27].

Previous Work at ISU

The first attempt at performing NR with the ISU UTR-10 Research Reactor was done by Dr. Robert Williams and Dr. Joseph Gray. In the fall of 1987, it was determined that the neutron flux emerging from the top beamport (created by removing the shield plugs from the top closures of the reactor) was sufficient to perform NR at reactor powers of one kilowatt.

The neutron and gamma radiation levels which accompanied the use of the open beamport at these powers required that there be biological shielding to reduce the radiation exposures in the unrestricted areas of the Nuclear Engineering Laboratory Building to an acceptable level. During the spring of 1988, two nuclear engineering seniors (Eric Pickel and Ed Wiegert) were charged with the design of a temporary biological shield which would allow routine experimentation with NR using the top beamport.

The temporary facility consisted of a collimator which is just the hole created by removing the plugs above the central vertical stringer in the reactor. The source size was assumed to be the four-inch by four-inch opening in the concrete near the core. The length (depth) of the collimator was 57 inches. In order to increase the neutron flux from the core, the 48-inch long graphite central vertical stringer was replaced with a 20 inch graphite stringer. The neutron flux in the beam at the reactor power of one kilowatt was 4.0×10^6 neutrons/cm^2*sec. The shielding for the temporary facility consisted of four inches of lead in the form of blocks around the beam path and a seven inch thickness of concrete blocks around the lead. In the direct path of the emerging beam, there were six inches of paraffin sandwiched by boral plates on the top and bottom to remove the neutron component of the beam. The shield was topped by four inches of lead and seven inches of concrete. The shielding reduced the exposure in the unrestricted areas of the Nuclear Engineering Laboratory Building to acceptable levels. The position of the temporary facility is shown in Figure 1.2 and the design of the shielding is shown in Figure 1.3.

After the temporary facility was assembled, it was used to produce neutron radiographs of simple objects such as an aluminum block with milled slots, HN to BNC coaxial cable connectors, and a cigarette lighter. From the initial radiographs, it was determined that NR was feasible using the top beamport. However, the images produced using the top beamport left much to be desired. Since NR has been done at similar reactors with much better results [28,29,30,31], the key to improving the the image quality was through increased collimation. This was the path chosen to improve the quality of the neutron radiographs produced using the UTR-10 reactor.

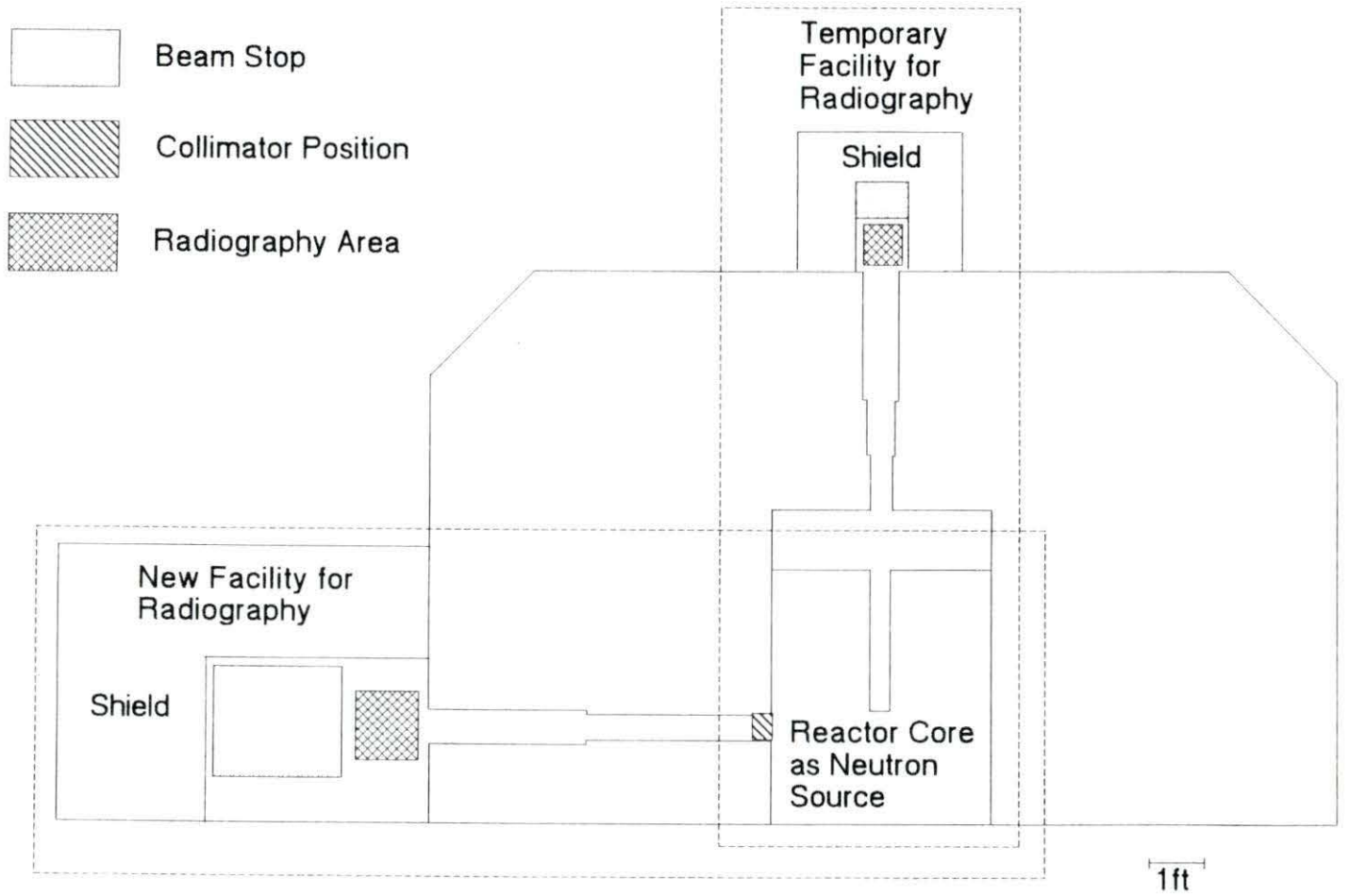

Figure 1.2: The Layout of the Two Neutron Radiography Facilities

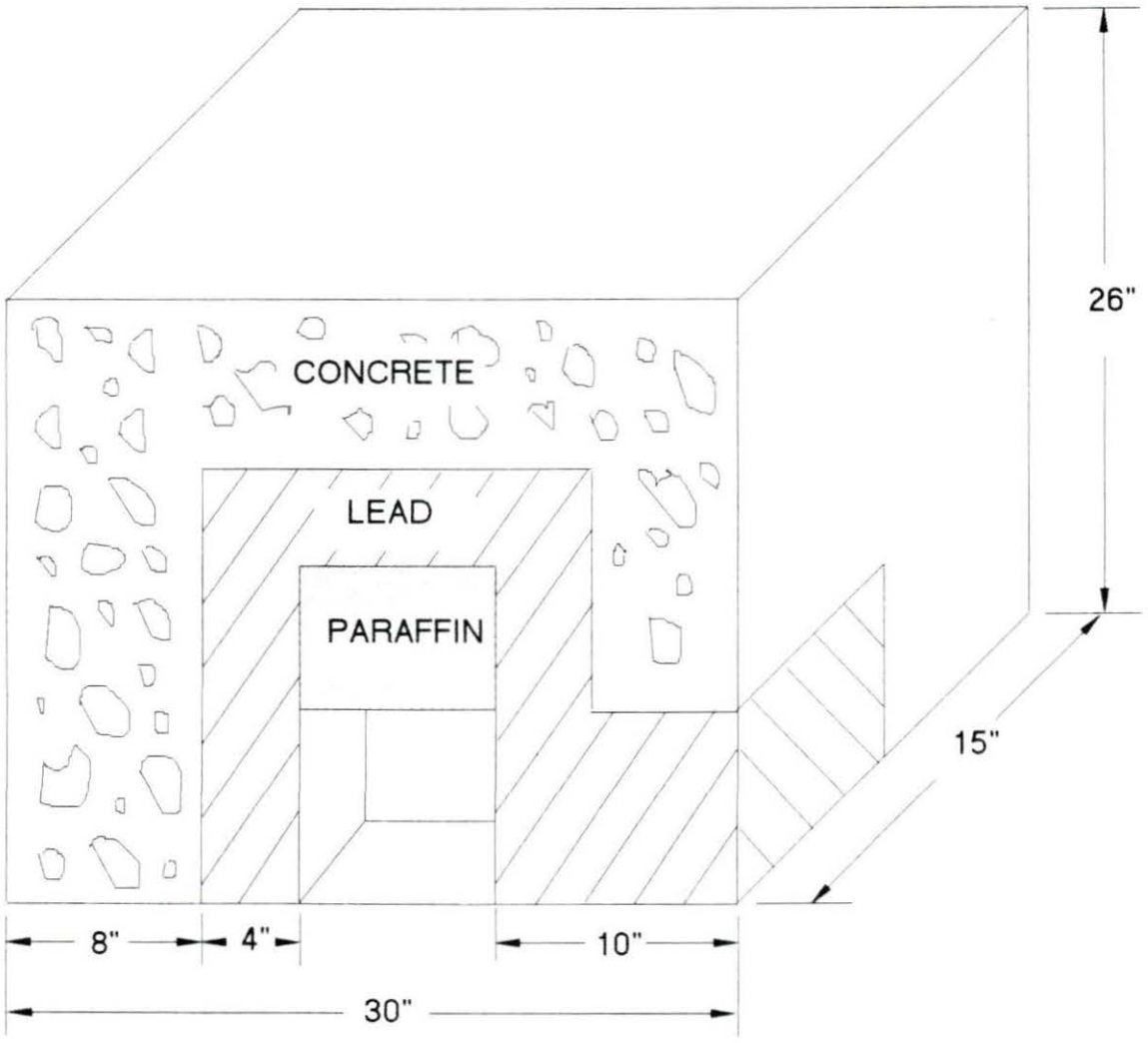

Figure 1.3: A Cut-Away of the Temporary Facility's Shielding

CHAPTER 2. BACKGROUND AND THEORY

Necessities for Neutron Radiography

There are four things necessary for NR: a neutron source, a method to define a beam of neutrons (collimation), an object to be examined, and a method to record the information conveyed in the spatially varying intensities in the transmitted neutron beam [2,4,5,6,7,32,33].

Sources

There are four types of neutron sources that have been used for NR: Accelerators, spontaneous fission sources (californium), alpha-neutron reactions (plutonium-beryllium) and reactors. The neutrons from all these sources are born with energies far in excess of those desired for thermal neutron radiography. The neutrons need to be slowed from high energies ranging from 1 MeV to 14 MeV, depending on the source, to around 0.02 eV to enhance the difference in neutron attenuation between the different materials that make up the samples. During the slowing down process, neutrons are lost by absorption in the moderating material and by scattering out of the beam. The higher the energies that the neutrons are born with, the greater the loss of neutrons from the source.

Each type of source has advantages and disadvantages. Accelerators and reactors can produce large collimated neutron fluxes (on the order of 10^6 to 10^8 neutrons/cm^2*sec at the detector) which allow short exposure times. Reactors and accelerators are not portable and require large

capital expenditures. Spontaneous fission and alpha-neutron sources generally have much lower collimated neutron fluxes (on the order of 10^4 to 10^5 neutrons/cm^2*sec at the detector), but their small sizes make them portable which allows neutron radiographs to be taken where the part is used [4,5,6,32,33,34].

Collimation

Collimation is important in improving the quality of the image produced which, in turn, increases the information that can be inferred from the radiograph. The collimation of the neutrons can be achieved by two methods, parallel plate collimation and divergent collimation. The number of collimation methods are limited since the only way to control the direction in which neutrons travel is by controlling the source geometry from which they diverge or by removing the neutrons which are not traveling in the desired direction [2,4,5,32,33,34,35]. The parallel plate collimator is shown in Figure 2.1 and the divergent collimator is shown in Figure 2.2.

The parallel plate collimator is essentially a series of plates of neutron absorbing material which remove the neutrons which are not traveling parallel to the plates providing a mono-directional plane source. This method is losing favor as it reduces the neutron flux available for radiography.

The other method of defining a beam of neutrons is to define a source geometry. This method of collimation is easy to obtain by just placing neutron absorbing material in such a manner that neutrons emerge from only a small area. As the distance between the source and the object under investigation becomes larger, the source can be approximated by a point source. The geometric unsharpness is reduced as the ratio of the distance between the source and object divided by source size is increased. Figure 2.3 shows geometric unsharpness and

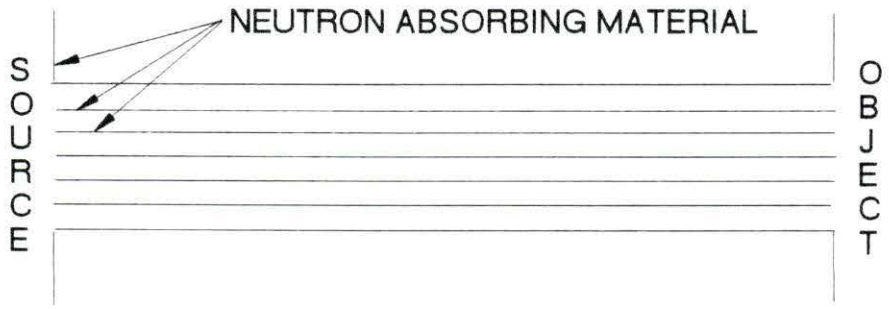

Figure 2.1: Parallel Plate Collimator

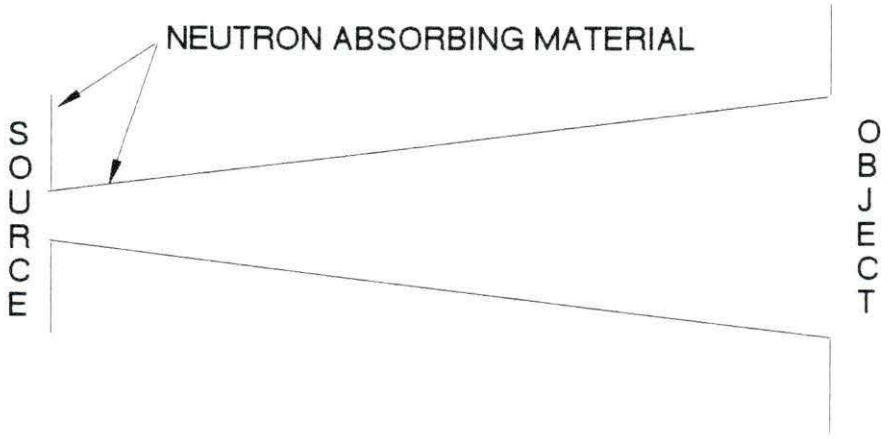

Figure 2.2: Divergent Collimator

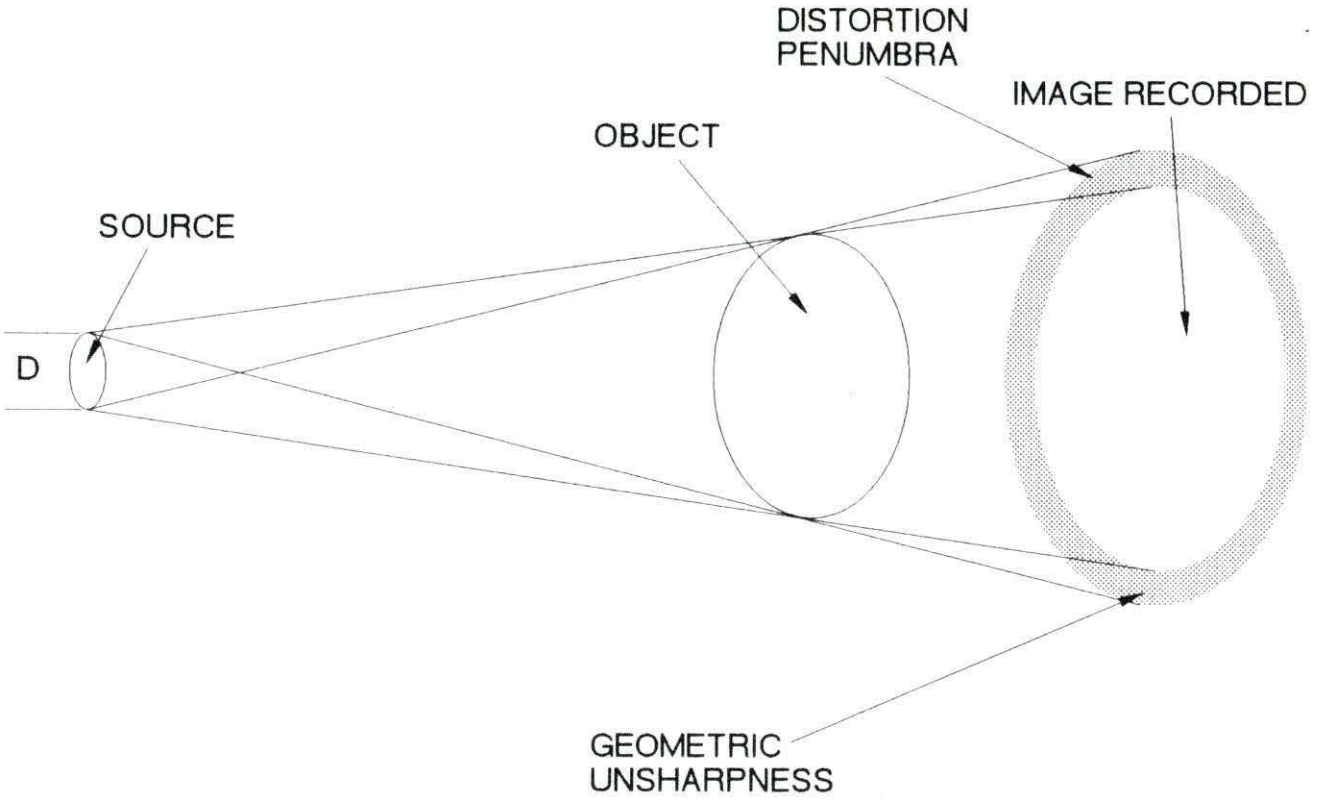

Figure 2.3: Geometric Unsharpness

how it affects the image of the flaw as it would appear on the film. The problem arises as the neutrons from one side of the source cast the shadow of the flaw in a slightly different position than the neutrons from the other side of the source. As the shadow that is cast becomes less defined, the resulting contrast in the film decreases, which reduces the chances of detecting the flaw.

Detectors

Since neutrons are a very penetrating and nonionizing form of radiation, their detection is a complicated process. There are four methods used to convert the transmitted neutrons into a form of radiation that can be recorded. Most methods use elements with large neutron absorption cross-sections like indium, cadmium, boron, gadolinium, or dyprosium in order to efficiently convert the neutrons to a form of radiation that is easier to detect [2,4,5,7,32,33].

The transfer method uses a metal foil that becomes activated and decays emitting beta and gamma rays in proportion to the neutron flux transmitted through the object. The activated foil is then placed in contact with x-ray film. The induced radioactivity in the foil exposes the film, thus "transferring" the image. This method has the advantage that it can be used in the presence of a large gamma radiation field and uses relatively common and inexpensive materials like indium for the activated foil.

The direct method uses a metal foil (usually gadolinium) that promptly emits an electron and/or gamma ray upon neutron absorption. This radiation exposes the film which is in close proximity to the conversion foil. This method requires that the gamma radiation is only a small portion of the beam; otherwise the film will be exposed by the gamma radiation and not the radiation produced by the conversion foil. The low gamma component of the beam is usually produced at the expense of the intensity of the neutron beam, because materials that attenuate gamma rays will also attenuate the neutrons.

The track etch method uses a material, boron or lithium, which promptly produces an alpha particle upon absorption of a neutron, which leaves a track in the film. The method has the advantages that it can be done with a large gamma radiation field and does not require a darkroom to develop the film. The image is revealed when the film is etched with acid.

Real time neutron radiography is emerging as the newest method. It requires an element that emits an electron upon absorption of a neutron, the electron then interacts with a phosphor producing a photon that is recorded by a television type camera. This method is very expensive and usually requires a low gamma component of the radiation field [5,32].

Parameters of Interest for Neutron Radiography

The parameters of interest for NR are the effects due to using a finite extended source which causes unsharpness or blurring of the image. This parameter, the geometric unsharpness, is essentially the distance between the source and transfer foil divided by the source diameter and it places an absolute limit on the size of flaw can be detected. Other parameters of interest deal with the distribution of neutron energies, the effects scattered neutrons have on the image, and unsharpness not caused by geometry alone.

The neutrons which leak from the reactor are distributed with a range of energies. The neutron cross-sections of the materials under investigation, as well as the transfer foil, depend on the neutron energy. The isotope used to transfer of the image, indium-115, has several large neutron absorption resonances in the epi-cadmium energy region. (The term epi-cadmium indicates that the neutrons are of energies greater than 0.5 eV.) Absorption of neutrons of energies corresponding to these resonances could possibly account for a measurable portion of the film density recorded on the film. This portion of the film density shows the epi-cadmium and NOT the expected thermal neutron properties of the material under investigation. A

typical reactor spectrum is compared with the indium and cadmium absorption cross-sections and is shown in Figure 2.4. The important features of this diagram are the large indium resonances which represent an appreciable amount of possible epi-cadmium neutron absorption in the epi-cadmium energy region.

The third property of interest is the activation of the indium foil by neutrons which are scattered by the object under investigation. While the neutron scattering cross-section provides important information by attenuating the neutron beam, the scattered neutrons can eventually activate the indium foil. The image that is then transferred contains a uniform noise from the activity produced by the absorption of the scattered neutrons. The amount of this noise depends on the distribution of the scattering material, the scattering cross-section and the thickness of the materials under investigation.

The epi-cadmium and scattered neutron contribution to film density reduces the amount of contrast which can be used to record the different aspects of the object under investigation. Image processing techniques can be used to increase the contrast of the image on the film by subtracting the background film density due to the activity from the epi-cadmium and scattered neutrons and then "stretching" the image contrast.

There are also parameters of lesser impact which deal with just the transfer of the image from the indium foil to the film. One parameter is the amount of exposure of the film due to each of the beta and gamma radiations produced by the decay of the indium. The high attenuation of the beta particles (with the accompanying large energy deposition) exposes the film much more effectively than the gamma radiation. The shielding of the beta particles by the film packets and film itself creates a rapid decrease in exposure which can limit the use of multiple films to record the image.

There is another contribution to the unsharpness which occurs when the transfer method of

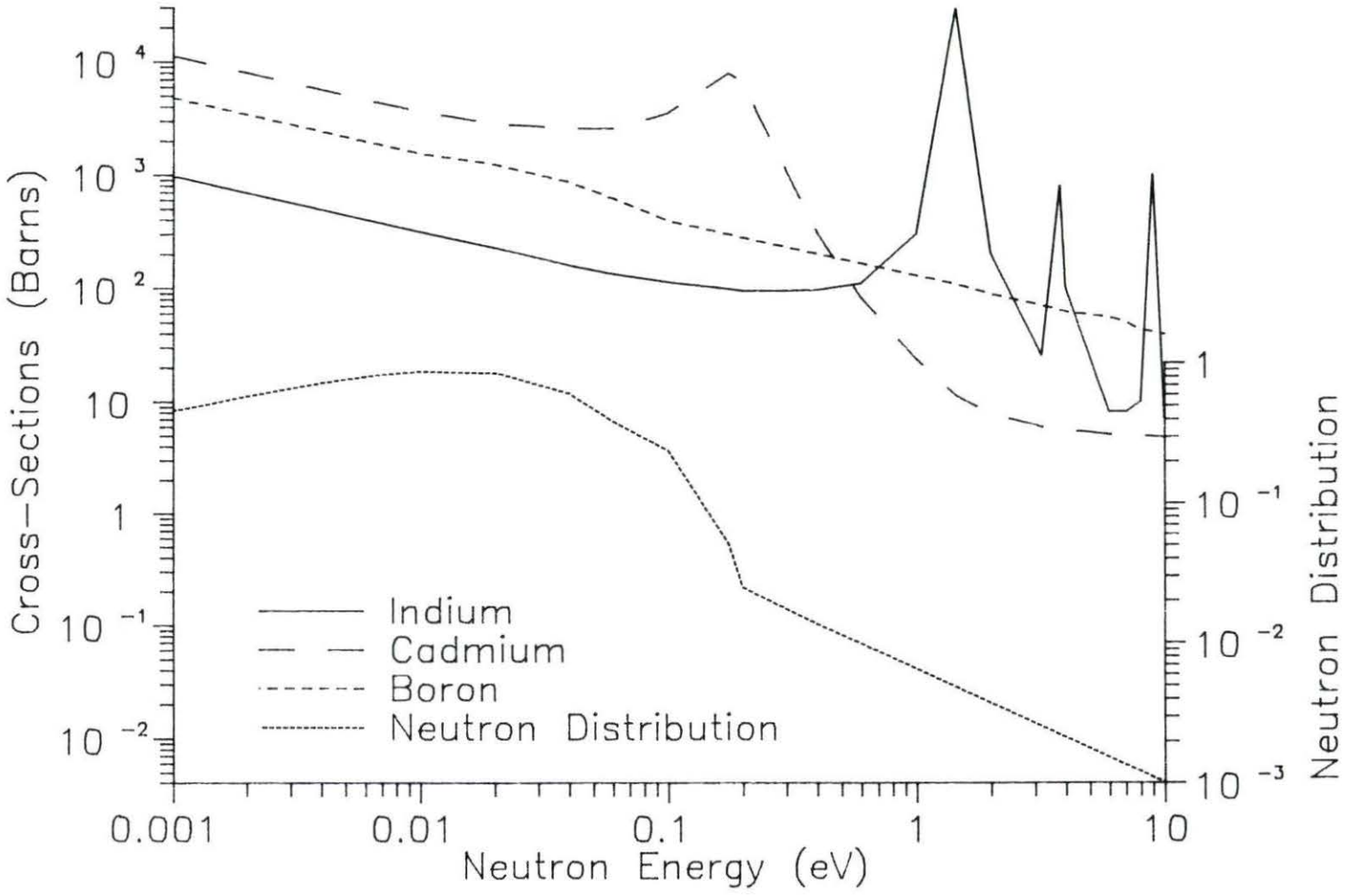

Figure 2.4: Neutron Cross-Section and Neutron Energy Distribution vs Neutron Energy

NR is used. The problem arises from the spreading of the image by the radial divergence of the radiation from the indium foil which transfers the image. The amount of this unsharpness can be reduced by decreasing the distance between the film and foil, but there is always a distance between the two due to the finite thicknesses of the x-ray film, the transfer foil, and the packet the film is in to prevent the film from being exposed by the light.

The last parameter investigated is the film unsharpness. This is due to the secondary electrons traveling away from the original site of the incident radiation's interaction with the film material. This parameter should not be significant when compared to the geometric unsharpness and the transfer unsharpness.

Film-Foil-Object Transfer Model

This model assumes that the neutrons are in a beam which has the neutrons traveling perpendicular to the indium transfer foil and object. The greater the degree of collimation and the closer the sample under investigation is to the indium foil, the better the approximation holds. The neutrons are assumed to be thermal and the nuclear properties are taken at this energy. The scattered neutrons are assumed to be scattered uniformly by the object and contribute to a uniform activation of the indium transfer foil producing a uniform contribution to the film density. The conversion foil is assumed to be thin and of uniform thickness.

The thermal neutron absorption cross-section that produces the In-116m_1 isomer, used to transfer the image is 162.5 barns [37]. The half-life of In-116m_1 isomer is 54.15 minutes which allows plenty of time to remove the indium foil and transfer the image.

The neutron flux that is transmitted through the object depends upon the cumulative macroscopic neutron scattering and absorption cross-sections in the object along the path that the neutrons travel through the object. The equation that describes the resultant neutron flux

after transmission through the object is Equation 2.1.

$$\Phi(x,y) = \Phi_0 \exp\left[- \sum_{i}^{n} \left(N_i(x,y) \left(\sigma_{ai} + \sigma_{si} \right) \right) \right] + \Phi_s \qquad (2.1)$$

Where:

Φ = Neutron Flux After Interaction With The Object
Φ_0 = Neutron Flux Before Interaction With The Object
Φ_s = Scattered Neutron Component of The Beam
N_i = Number of Atoms of Each Element in The Neutron Beam Path
y = Vertical Position in The Neutron Beam
x = Horizontal Position in The Neutron Beam
σ_{ai} = Elemental Neutron Microscopic Absorption Cross-Sections
σ_{si} = Elemental Neutron Microscopic Scattering Cross-Sections
i = Individual Element Subscript
n = Total Number of Elements in Beam Path

The activation of the transfer foil depends on the thickness, density, absorption cross-section, and half-life of the foil material, as well as the time of exposure and the neutron flux that is transmitted through the object. The simplified equation for the activity at a point on the transfer foil is given in Equation 2.2.

$$A(x,y) = N_f \sigma_{af} \Phi(x,y) \left(1 - \exp(-\lambda_f t_{irr}) \right) \qquad (2.2)$$

Where:

Φ = Neutron Flux After Interaction With The Object
A = Activity of Transfer Foil Due to Absorption of Neutrons

λ_I = Decay Constant of Isotope Transferring the Image
N = Number Density of Element Transferring the Image
y = Vertical Position in The Neutron Beam
x = Horizontal Position in The Neutron Beam
σ_{al} = Neutron Microscopic Absorption Cross- Section of Foil
t_{irr} = Time of Irradiation of The Transfer Foil in The Neutron Beam

The exposure of the x-ray film by the transfer foil producing the image depends on the activity and half-life of the transfer foil, the time of the exposure, and the time between the foil activation and film exposure. The equation that governs the exposure of the x-ray film (assuming that the foil and film are in direct contact) is shown in Equation 2.3.

$$\Psi(x,y) = 0.5A(x,y)\left(\exp(-\lambda_I t_w) - \exp[-\lambda_I(t_w + t_{ex})]\right) \qquad (2.3)$$

Where:

Ψ = Exposure of The X-Ray Film Due to The Decay of The Transfer Foil
A = Activity of Transfer Foil Due to Absorption of Neutrons
λ_I = Decay Constant of Isotope Transferring the Image
y = Vertical Position in The Neutron Beam
x = Horizontal Position in The Neutron Beam
t_w = Time Between Irradiation of The Transfer Foil And Exposure of Film
t_{ex} = Length of X-Ray Film Exposure

The model for the density of the x-ray film depends upon the film properties of fog density, noise, maximum film density and the interaction cross-section of the film to the beta and gamma radiations as well as the radiation fluence. The equation that describes the film density as a function of position is Equation 2.4. The approximations made for this equation are better

when the film is close to the decaying foil and the smaller the amount of shielding between the foil and film.

$$D(x,y) = D_0\left[1 - \exp(-\sigma_x[\Psi(x,y) + \delta])\right] \qquad (2.4)$$

Where:

- D = The X-Ray Film Density
- D_0 = The Maximum X-Ray Film Density
- Ψ = Exposure of The X-Ray Film Due to The Decay of The Transfer Foil
- σ_x = The X-Ray Interaction Cross-Section of The Film
- y = Vertical Position on The Transfer Foil
- x = Horizontal Position on The Transfer Foil
- δ = The Film Fog Density

CHAPTER 3. FACILITY DESIGN

Criteria

The major criteria for design of the components were effectiveness, cost, and low activation of the materials used. The major goal of the total shielding was to reduce exposures in the unrestricted areas of the Nuclear Engineering Laboratory Building to under two millirem in any hour to comply with 10 CFR 20 in the Code of Federal Regulations [38]. The costs of some materials were not considered as they were windfalls from past projects. For example, the indium foils used to transfer the image were left over from previous neutron radiography experiments carried out with the Ames Lab Research Reactor.

The use of low activation materials is especially important in the collimator since the thermal neutron flux is estimated to be $3x10^{10}$ neutrons/cm^2*sec in the collimator region. The estimation of this flux comes from extrapolating measured neutron fluxes at a reactor power of 500 watts to ten kilowatts, the expected reactor power for NR. The estimated neutron flux at full power was then used in Equation 3.1, given in Schaeffer [39], to estimate the line of sight flux at the source in a circular port.

$$N = \frac{2\Phi}{\ln\left[1 + \left(\frac{a}{z}\right)^2\right]} \qquad (3.1)$$

Where:

Φ = Measured Neutron Flux
N = Estimated Neutron Flux
a = Diameter of Source
z = Length of Port

The cost limitation was due to the size of the grant available for the project. The amount of money allocated did not allow much beyond function. Many of the items manufactured, like the beamstop, were home-made to save on labor costs. The material and manufacturing costs (when applicable) for each item are given in Appendix B. Some of the funding for purchasing the needed materials as well as x-ray film, facilities and the equipment for analyzing the radiographs were provided by the Center for Nondestructive Evaluation.

The west beamport was chosen as the site for the improved facility because the distance between the neutron source and the indium foil recording the image would be increased over the position of the temporary facility. The ratio of the distance between the source and indium foil to the diameter of the source (L/D) is an important measure in determining the absolute limit on the ability to detect aspects under investigation in the object. The ratio is also a common feature used to compare facilities for NR. By using the west beam port and the collimator, the L/D is triple that of the temporary facility on the top.

The west side of the reactor had plenty of room to construct the shielding without interfering with the normal operation of the reactor. The extra area to work with also allows the effective distance from the source to be increased by placing the radiography setup farther from the beamport. There was also some worry about the weight of the shielding upon the top of the reactor which could be better supported by the reactor room floor. The possibility of dropping materials into the reactor core is also eliminated as the west beamport is horizontal

instead of vertical.

The transfer method was chosen to take the neutron radiographs since there is a large gamma flux accompanying the neutrons in the beam which would expose the film if the direct method were to be used. Also, indium foils which could be used to transfer the image in the transfer method were already available. The transfer method allows the design of the collimator to be concerned only with improving the recorded image by defining a small source size.

Collimator

The ultimate factor for resolving the aspects of an object under examination is the geometric unsharpness. In order to decrease the unsharpness, the source size for neutron radiography using the west beamport should be as small as possible. The source size was determined by calculating the smallest allowable size that would still provide the necessary neutron flux to produce the radiographs with the same foil activation as previously achieved using the temporary facility. The necessary run time was chosen to be the same as that of the temporary facility in order to produce a radiograph in a reasonable amount of time. The reactor power was chosen to be the maximum power allowable, to use as small of a source size as reasonably possible. The short neutron exposure time of twenty minutes allowed room for error in case the calculations were wrong on either the neutron flux or shielding. If the neutron flux was low, the exposure times could be increased. If the shielding was inadequate, the power could be decreased and exposure time lengthened. The calculation yielded a source size of 2.5 inch diameter circle.

There are six elements that have very favorable neutronic properties for defining a source size to collimate the neutrons and have been used by other sites investigating the use of neutron radiography; they are gadolinium, europium, dyprosium, cadmium, indium and boron [40]. The materials' costs and properties are given in Table 3.1. The six elements are compared on the

cost of the materials for a 99% attenuation of the incident neutrons. Indium, europium and dyprosium were not readily available or too expensive for the quantity needed to attenuate the neutron flux to the necessary level. The three elements which were available, affordable and had desirable neutronic characteristics were gadolinium, cadmium and boron.

Table 3.1: Collimator Materials and Costs (1990 Costs)

Material	Thickness for 99% Attenuation	Cost per cubic cm	Equivalent Shielding Cost
Boron Carbide	0.0560 cm	$ 0.40	$ 3.38
Cadmium	0.0404 cm	$ 0.71	$ 4.34
Dyprosium	0.1530 cm	$ 12.62	$ 291.07
Europium	0.0517 cm	$ 159.3	$ 1241.51
Gadolinium	0.0033 cm	$ 14.63	$ 7.28
Indium	0.6308 cm	$ 6.49	$ 617.25

Gadolinium was not chosen due to the lack of information on the chemical compatibility with the rest of the materials used in the collimator. Also, the small thickness of gadolinium necessary, 0.0033 cm, could complicate the construction of the collimator since rolling a uniform gadolinium foil that thin could be a problem.

Boron carbide, B_4C, was chosen over cadmium because the epi-cadmium neutron absorption cross-section is much higher. Since a large component of the image recorded is due to the epi-cadmium resonances in the indium foil, the epi-cadmium neutrons also need to be removed.

Another factor which makes boron carbide better suited for the collimator than cadmium is that the boron neutron capture products are not radioactive. Boron carbide was chosen as the

material form since it has a very high boron content and is extensively used in combination with epoxy as a solid shapeable neutron absorbing material. The source size was reduced from six inches in diameter to 2.5 inches in diameter by a washer-shaped disk 0.25 inches thick to guarantee that no inhomogeneities would allow neutrons to pass through.

Lead, in the form of an annulus four inches long with a six inch outer diameter and a 2.5 inch inner diameter, was placed behind the boron carbide to reduce the gamma ray dose which accompanies the neutron beam. The collimator is shown in Figure 3.1. Lead was chosen because of its low neutron absorption cross-section which results in low radioisotope production. The two isotopes of concern in lead are Pb-205 and Pb-209. The entire collimator and lead shielding is encased in aluminum to protect the materials which constitute it, as well as to make it easier to handle. The properties of the collimator materials are given in Table 3.2.

Table 3.2: Properties of Collimator Materials (from Nuclides and Isotopes [41])

Isotope	Abundance	Cross Section	Half Life	Stable End Product
B-10	0.199	3838 b		Li-7
B-11	0.801	0.005 b	20.20 ms	C-12
C-12	0.989	0.0035 b		C-13
C-13	0.011	0.0014 b	5730 a	N-14
Al-27	1.00	0.233 b	2.25 m	Si-28
Pb-204	0.014	0.86 b	1.5E7 a	Tl-205
Pb-206	0.241	0.03 b		Pb-207
Pb-207	0.221	0.7 b		Pb-208
Pb-208	0.524	0.0005 b	3.25 hr	Bi-209

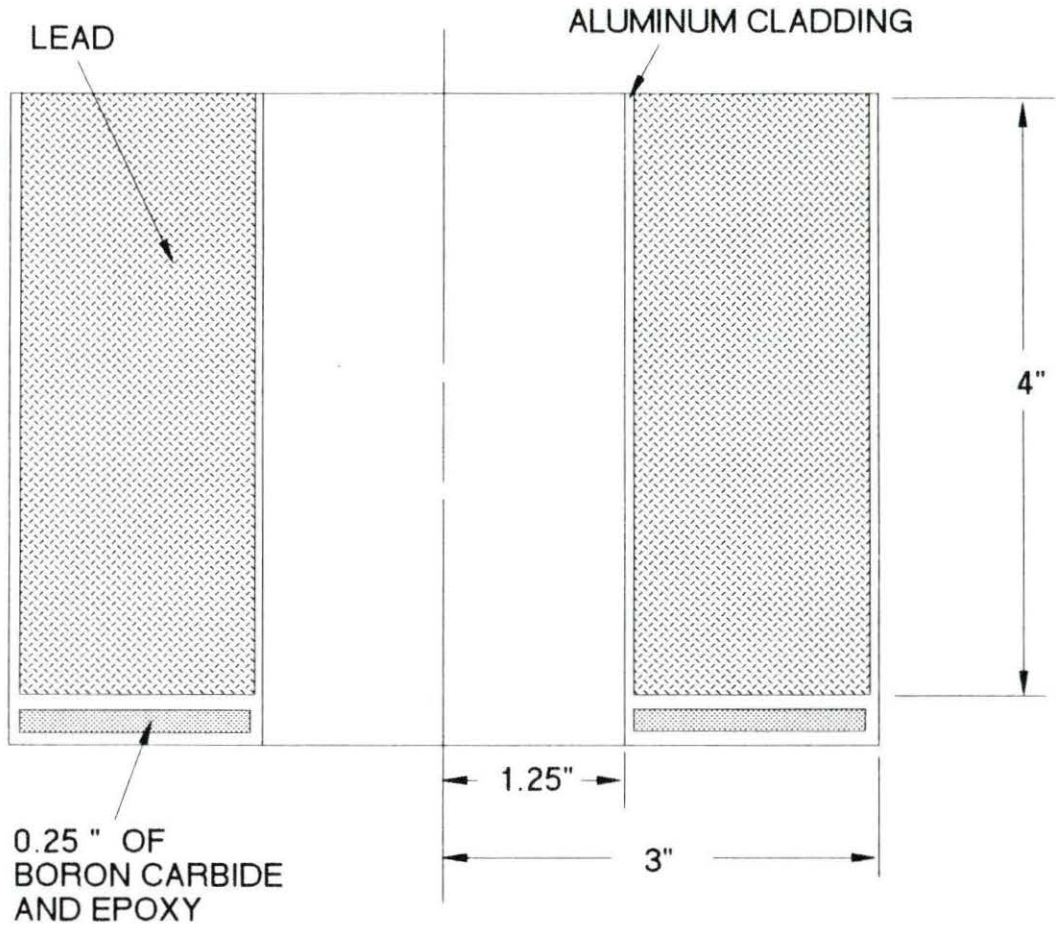

Figure 3.1: Cut-Away of Collimator and Lead Shielding

The collimator is installed in the beamport by using two sections of pipe, which are coupled together to allow a 2.5 inch bushing to be threaded into the collimator. The two sections of pipe can be disconnected so that placement and removal of the collimator can be done without removing more than the beamstop, and the large concrete shielding blocks which serve as a lid to the facility.

Beamstop

The fast neutron removal cross-section given by Blizard [42] was used to approximate the thickness of paraffin necessary to thermalize the fast neutrons that emerge from the core. The boric acid was added to capture the thermalized neutrons as well as capture to the thermal neutrons that are not stopped by the object and indium transfer foil. A thickness of eighteen inches of paraffin is used to thermalize the fast neutrons and is loaded with five percent boric acid by weight to absorb the thermalized and thermal neutrons from the beam. The actual beamstop surface which first contacts the beam is recessed six inches into the beamstop to reduce the neutron backscatter, which could add noise by activating the indium transfer foil. The boric acid and paraffin mixture was melted and poured into a wood frame box. This box was constructed using wooden pegs and glue to reduce the chance of activating the nails or screws which could have been used. The beamstop is shown in Figure 3.2.

The beamstop is placed using ropes wrapped around both ends to create a place for the crane to hook and lift. The ropes are removed to reduce the possible activation of the rope and replaced with twine to allow the ropes to be rethreaded around the beamstop for removal without disassembling the concrete shielding.

Concrete Biological Shielding

There are two feet of concrete shielding perpendicular to the neutron beam around the radiography area and beamstop. The two foot thickness of concrete was determined by

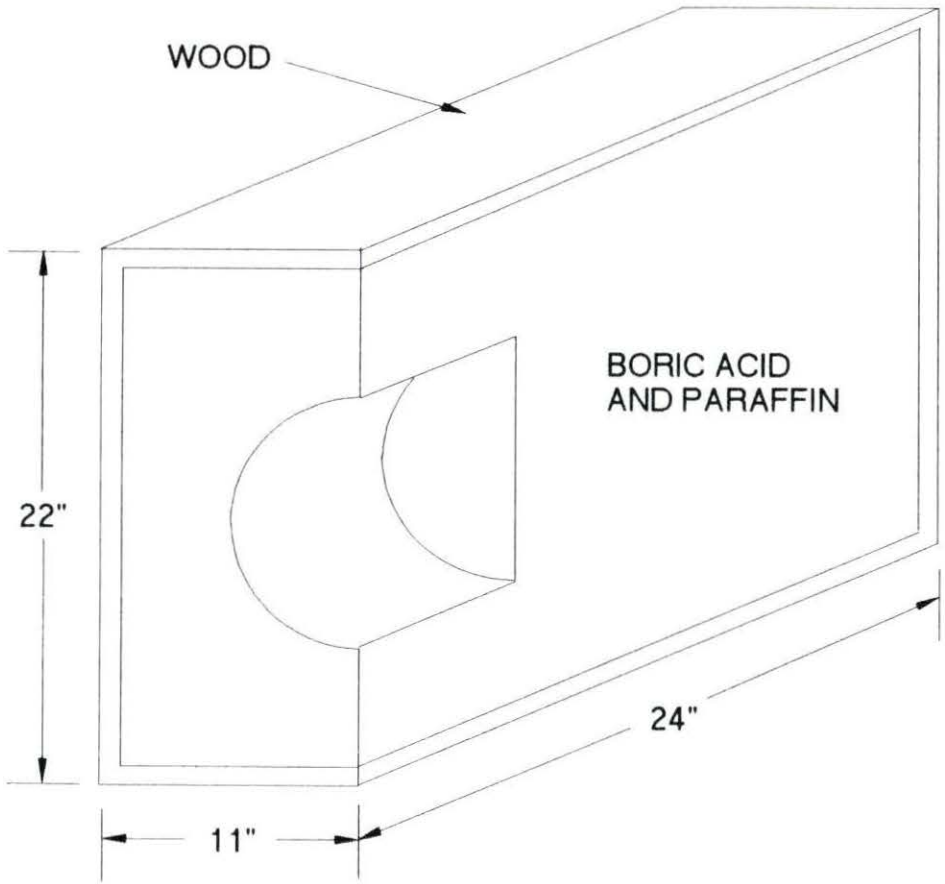

Figure 3.2: Cut-Away of Neutron Beamstop

approximating the capture gamma source as a point source in the center of the beamstop, which is shielded by the concrete, using the Berger Build-up factor for a point isotropic source given by Lamarsh [43]. The 4.47 and 4.73 MeV prompt neutron capture gammas given by Blizard [42] from boron-10 were used as the energies of the point source. The dose that was used to determine the thickness of the shield was 2 mR/hr at the closest point to the beamstop on the external surface of the concrete.

The three foot thickness of concrete behind the beamstop was determined by extrapolating dose vs concrete thickness measurements made while at different reactor powers on the top of the reactor. The layout of the concrete shielding is given in Figures 3.3 and 3.4.

Administrative Controls

For safety reasons, the design and use of the facilities for NR had to be approved by the proper University Committees. The original shield design proposal was reviewed and approved by the Reactor Use Committee on November 17, 1989. After completion of the shield construction, the procedures for use and testing of the shielding were reviewed and approved by the Reactor Use Committee. The procedures for handling and use of the radioactive materials (mainly the indium transfer foil) were reviewed and approved by the University Radiation Safety Committee. The major stipulations required for operation were that the facility be monitored and surveyed by a health physicist when operated, and that the health physicist be informed of the expected activity of the samples and foils which were used for NR.

The survey of the shield indicated that there would not need to be a limit on run time or reactor power, as the dose in the unrestricted areas of the Nuclear Energy Laboratory was well below 2 mr/hr. The shielding functioned as well as expected, except for neutron leakage where the shielding butts against the reactor shield. The leakage was reduced by adding a one-sixteenth-inch thick sheet of cadmium along the top edge of the shield at the reactor shield

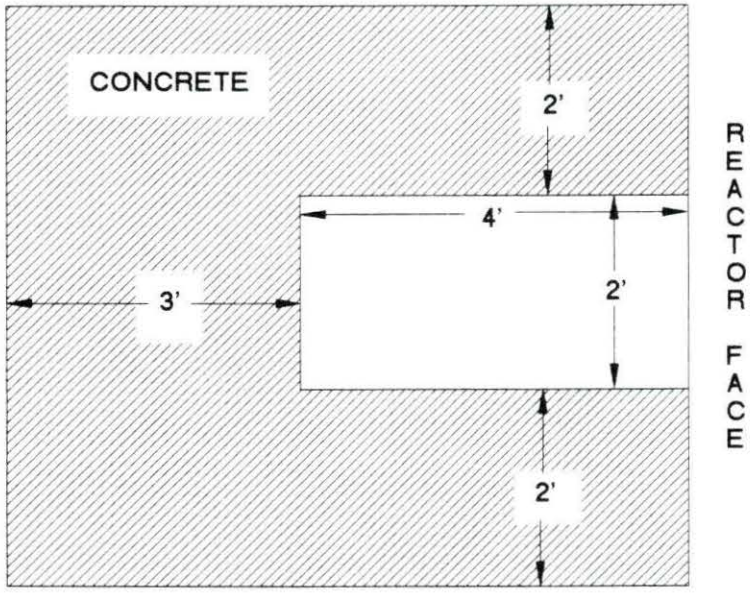

Figure 3.3: Top View of Concrete Shielding

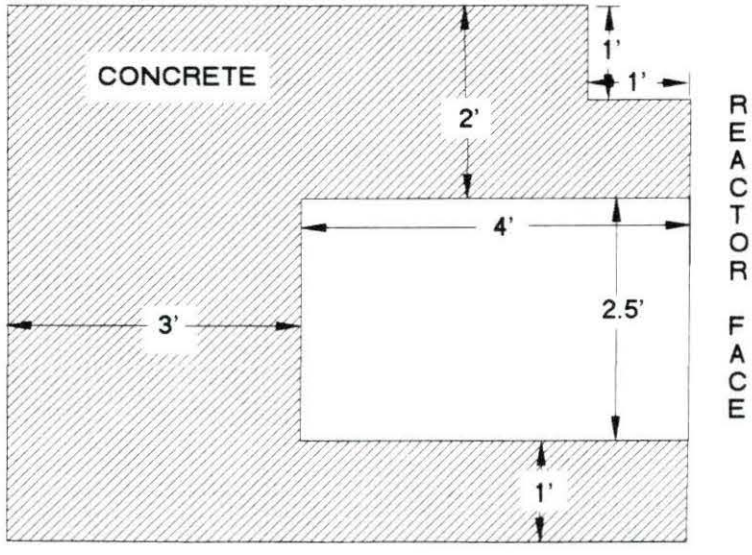

Figure 3.4: Side View of Concrete Shielding

interface. The dose from the prompt capture gamma of the cadmium was reduced by using lead blocks along the same crack. The health physicist's radiation survey of the shield with the reactor at full power is given in Appendix B.

The handling of the indium transfer foil should be done with long tongs under the supervision of a health physicist. The person handling the foil should also wear a ring dosimeter as the activity of the foil could be as high as 1.5 R/hr beta + gamma.

CHAPTER 4. NEUTRON RADIOGRAPHY USING THE UTR-10

Sample Positioning

The samples and indium transfer foil used for NR were positioned fourteen inches from the face of the reactor in the path of the neutron beam, with the transfer foil perpendicular to the beam. A concrete block was used to shim the sample into the beam vertically and center the sample in the beam. A wood block was placed on the the end of the concrete block closest to the beamstop. The wood block had grooves that were used to position the radiography samples with respect to the transfer foil. The aluminum support plate, which backed the indium foil, fit into the groove to maintain the vertical perpendicular positioning of the indium foil. The samples were taped to the wood block to guarantee the sample-transfer foil placement.

Once the samples and indium foil were in place, the shielding was replaced and the materials were logged in the Reactor Operations Log (ROL) and the Irradiation Log. These entries were used to keep track of the status of the reactor and the materials irradiated. The removal of the materials and their activities after irradiation in the neutron beam were recorded in these logs also. The radioisotopes produced, their half-lives and theirexpected activities were also recorded on the proper isotope production form.

Procedure for Neutron Radiography

The personnel needed to perform NR include, a reactor operator, a senior reactor operator (on call), a health physicist, and a crane operator. The health physicist was informed about the procedures and the expected activities produced in the radiography materials. The Health Physist also monitored the removal and use of the radio-isotopes. The reactor operator and senior reactor operator were needed to operate the reactor.

All of the radiographs taken during this investigation were produced by irradiation in the west beamport facility for twenty minutes at a reactor power of ten kilowatts. The combination of run time, reactor power and film exposure time produced a film density of approximately 2.0 (maximum film density = 5) on Kodak AA-1 x-ray film. This produced sufficient contrast to observe the aspects under investigation. The same film density could have been achieved by decreasing the reactor power and increasing the reactor run time; however, short high-power runs were used. The short high-power runs were chosen to reduce the time commitment for all the people involved.

The activity produced in an indium foil depends on the neutron flux and the length of the irradiation. The activity in the foil asymptotically approaches a maximum value that depends on the neutron flux. The asymptotic value is reached when the rate of decay of the indium-116m_1 isomer equals the rate of production. Since the neutron flux available for NR increased linearly with reactor power, the minimum reactor power necessary to produce a film density of 2.0, with a 0.01 inch thick indium foil and Kodak AA-1 x-ray film, was 2.25 kilowatts. The relation between reactor power and the production of activity in the foil is indicated in Figure 4.1. Activation of the sample for longer than four half-lives (3.6 hours) would not yield much added activity, as 93% of the possible activation would be achieved by

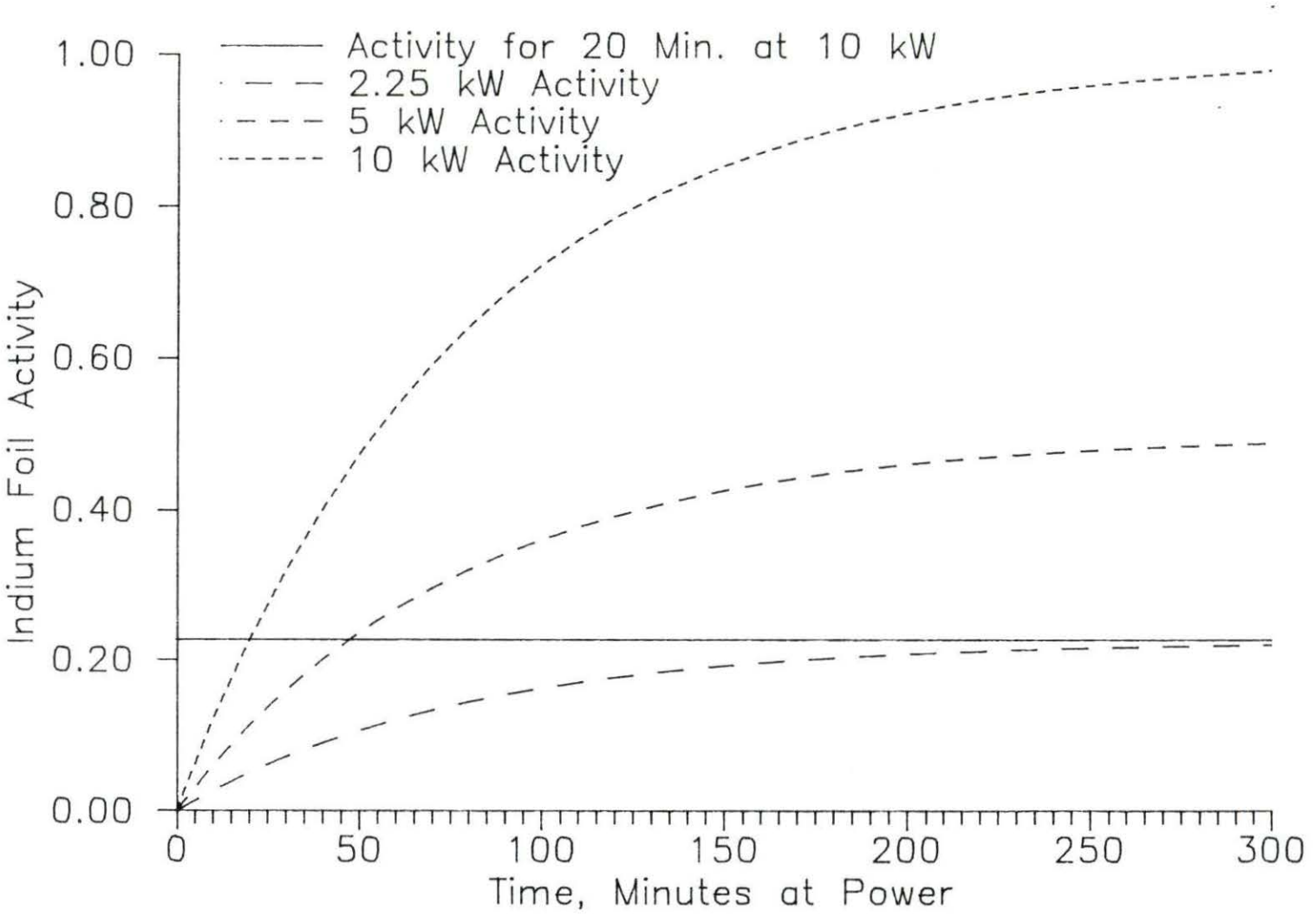

Figure 4.1: Reactor Run Time vs Indium Activity (Normalized to 10 kW Saturation)

then. The use of a faster film would allow lower reactor powers or shorter run times to produce the same film density, as faster films require less radiation to achieve a given film density.

After the irradiation, the indium foil and aluminum support plate remained in the concrete shielding for approximately 20 minutes to allow the short lived activation products in the sample and transfer foil to decay. This reduced the exposure due to short lived activation products to the person handling the foil and the x-ray film. The short lived activation products would add unwanted exposure to the x-ray film which would decrease the dynamic range of the x-ray film. The concrete lids and indium transfer foil were moved under the supervision of a health physicist who measured the beta and gamma doses. The sample and wood foil holder were also removed and their activities measured. Once the concrete shielding was replaced, the reactor configuration and the activities of the materials removed were logged in the Reactor Operation Log and Irradiation Log. The activity in the indium foil was as high as 1.5 R/hr beta + gamma on contact upon removal from the shield. The induced activity in the indium foil decayed away exponentially with a half-life of 54.1 minutes.

In order to transfer the image, the indium transfer foil was placed in contact with x-ray film in a light-tight paper package. The x-ray film and the indium transfer foil were then placed between lead sheets to reduce exposure to the persons working in the general vicinity. The x-ray film was thus exposed as the indium-116m_1 isomer decayed. The exposure was overnight but after the first four hours over 93% of the total possible exposure had been achieved.

Black construction-paper was chosen for the x-ray film packets to increase the film exposure due to the beta particles produced from the decay of the indium-116m_1 isomer. Using another material for the film package may have shielded the film from a large potion of the activity which transfers the image.

After exposure, the x-ray film was removed from the indium foil and developed in a

darkroom. The image was then examined by comparing the differing optical densities of the image using a film densitometer and/or by digitizing the image.

CHAPTER 5. DETERMINATION OF PARAMETERS

As noted in Chapter 2 (Background andTheory), there are a number of parameters that can be used to characterize the quality of a NR facility. Parameters investigated dealing with the neutron beam include: the number of neutrons passing through the radiography area, their energy distribution, their effect on the foil used to transfer the image, and their degree of collimation. Parameters dealing with radiographic method include: the contribution to film density due to the different radiations from the decay of the indium foil, the unsharpness due to the indium foil transferring the image, and the unsharpness due to the transfer of the radiographic image from the indium foil to the x-ray film.

Neutron Flux

The neutron flux in the radiography area was determined by irradiating indium foils in cadmium and aluminum covers at the mouth of the beamport. The activities of the indium foils were measured using a 2x2 NaI detector and a multi-channel analyzer (MCA). The number of counts collected with the MCA in the net peak area (NPA) -- corresponding to the 1.293 MeV decay gamma of the indium-116m_1 isomer -- were recorded. The same setup was then used to determine the NPA of a calibrated sodium-22 source using the 1.274 MeV decay gamma. The source and foils were far enough away from the detector to give the same source-detector geometry, and the closely matched energies were used to maintain the same detector energy efficiency. The NPAs, times, weights and known activity are used in Equation 5.1 to

determine the thermal neutron flux activating the indium foil. To estimate the fast neutron flux, the thermal neutron absorption cross-section was replaced with the resonance integral value, 3200 barns, for neutron absorption cross-section from "Nuclides and Isotopes" [41].

$$\Phi = \frac{NPA_{In}Act_{Na}T_{Na}M_{In}\lambda_{In}}{Y_{In}NPA_{Na}m_{In}\sigma_{In}N_{av}\left[1 - e^{(-\lambda_{In}t_0)}\right]e^{(-\lambda_{In}t_1)}\left[1 - e^{(-\lambda_{In}t_2)}\right]} \quad (5.1)$$

Where:

Φ = Neutron Flux (neutrons/(cm^2*sec))
NPA_{In} = Number of Decays Recorded From Indium Foil
NPA_{Na} = Number of Decays Recorded From Calibrated Sodium Sample
Act_{Na} = Activity of Calibrated Source
λ_{In} = Decay Constant for The Indium- $116m_1$ Isomer
σ_{In} = Thermal Neutron Cross-Section for Producing Indium- $116m_1$
m_{In} = Mass of Indium Foil
M_{In} = Molar Mass of Indium
T_{Na} = Time of Count Collection of Calibrated Source
t_0 = Length of Irradiation
t_1 = Time Between Irradiation of The Indium Foil And Count Collection
t_2 = Length of Indium Decay Count Collection
Y_{In} = Yield of 1.29 MeV Gamma Ray from Decay Of the Indium-$116m_1$
N_{av} = Avagadro's Number

The thermal neutron flux corresponds to the flux calculated using the indium foils in aluminum covers. The fast neutron flux was calculated from the indium foils in the cadmium covers. The cadmium ratio is defined here as the ratio of absolute activity of the indium foils in aluminum covers to the absolute activity of the indium foils in cadmium covers. The cadmium ratio is important as the activity produced by epi-cadmium neutrons reduces the dynamic range

of the x-ray film by decreasing the contrast in the film density. The thermal flux was calculated to be 5.8×10^5 n/cm^2*sec; the fast flux 6×10^3 n/cm^2*sec. The cadmium ratio was 4.8.

Geometric Unsharpness, L/D

The geometric unsharpness was determined by analyzing the characteristics on radiographic images caused by the geometric unsharpness. The relationships between source size, object, umbra and penumbra are shown in Figure 5.1. The umbra and penumbra are the portions of the shadow cast by objects due to the finite size of the radiation source. The penumbra is the outside light gray area which was not clearly defined because a portion of the source was not totally eclipsed by the object. The umbra was the lightest portion of the image (on the film, which is a negative image) because the source is totally eclipsed by the object. The image was used to determine the L/D, as the distance between the cadmium wire and indium foil at which the umbra could not be determined is the L and the wire diameter is the D. The contrast between the umbra and the background film optical density should remain the same when the distance between the cadmium wire and foil is less than the L in the L/D. When the distance between cadmium wire and foil exceeds the L in the L/D, the contrast between the peak and background film optical densities should decrease with increasing distance.

From the physical geometry of the setup, the distance between image recording device divided by the source's diameter indicated an L/D of 37.6. To determine whether the L/D was actually this value, the value was checked using procedures similar to those given in ASTM Standard E 803-86 [44]. The ASTM standard defines methods for determining the L/D of a neutron beam used for neutron NR. The method used required cadmium wires, 0.064 cm in diameter, to be placed at fixed distances from the neutron image recording device, in this case the indium foil. The radiographic image of the cadmium wires was analyzed to determine the distance between the foil and the wire at which the umbra is no longer visible. The L/D is just

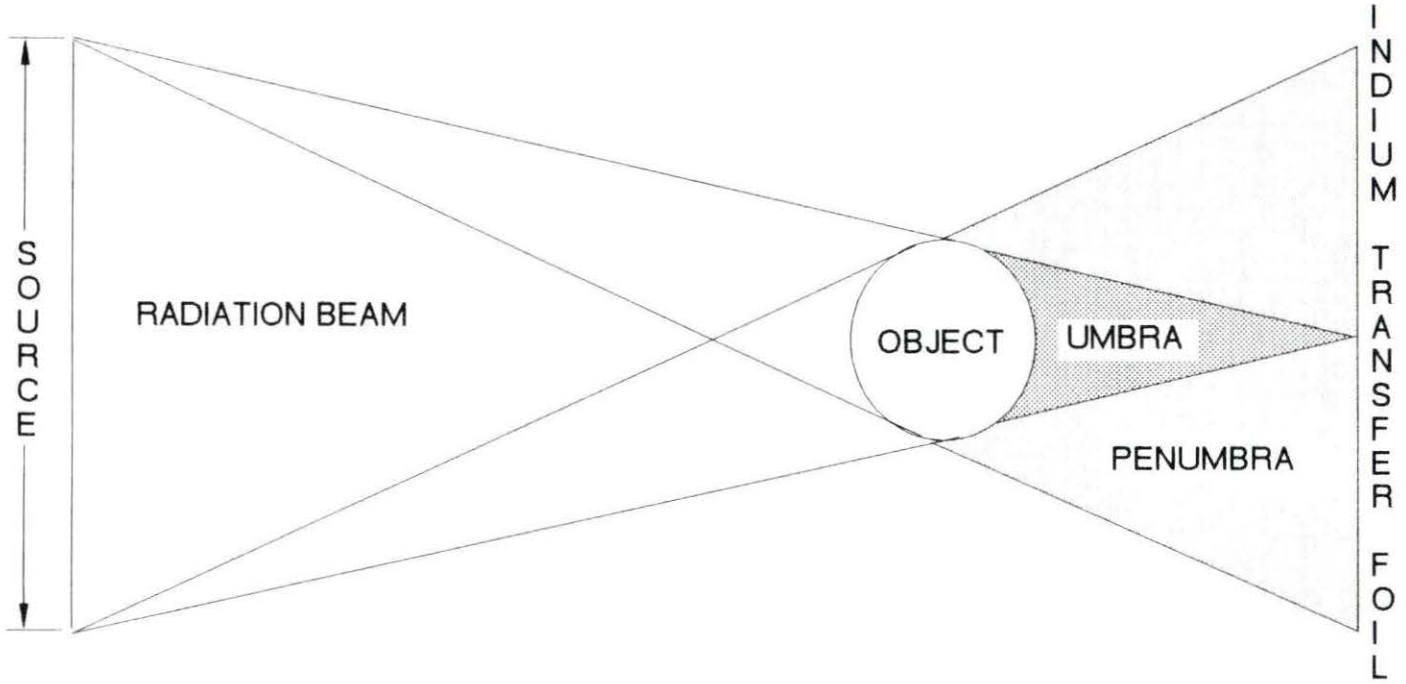

Figure 5.1: Umbra, Penumbra, Foil, Object, and Source Relationship

that distance divided by the wire diameter.

The equipment used for determining this parameter was 0.064 cm diameter cadmium wires mounted at 0.25 inch intervals along the length of an aluminum plate, which provided support and maintained the alignment of the wires. The entire assembly was then placed at a 45 degree angle to the indium transfer foil so that each wire was a known fixed distance from the foil. The setup for the L/D determination is shown in Figure 5.2.

The radiographs were taken at a position 14 inches from the opening of the beamport, a reactor power of 10 kilowatts and an activation time of twenty minutes. The foil was then used to expose the x-ray film overnight. After the film was developed, the image was magnified and digitized using a camera. The radiograph used for the L/D determination is shown in Figure 5.3. The separation distance between the cadmium wires and indium transfer foil increases from left to right.

The first inspection method was just to visually check the radiograph for the point at which the "white" umbra lines disappeared and were replaced by wider less bright lines. The greatest distance between the cadmium wire and the indium transfer foil which still has the umbra divided by the width of the wire is the L/D of the setup. This method gave an L/D of at least 35 but not more than 42.

To justify the visual inspection, slices of the digitized images were then taken perpendicular to the wire and averaged to reduce the local variations in the optical film density. Since the "background" film density recorded on the digitized images was not uniform, the background was averaged over the low film density "valleys." The background was determined by a straight line averaging between the background film densities on either side of the "valleys", corresponding to the cadmium wire. The differences in film density between different digitized images were normalized by comparing the area between the "valley" corresponding to the

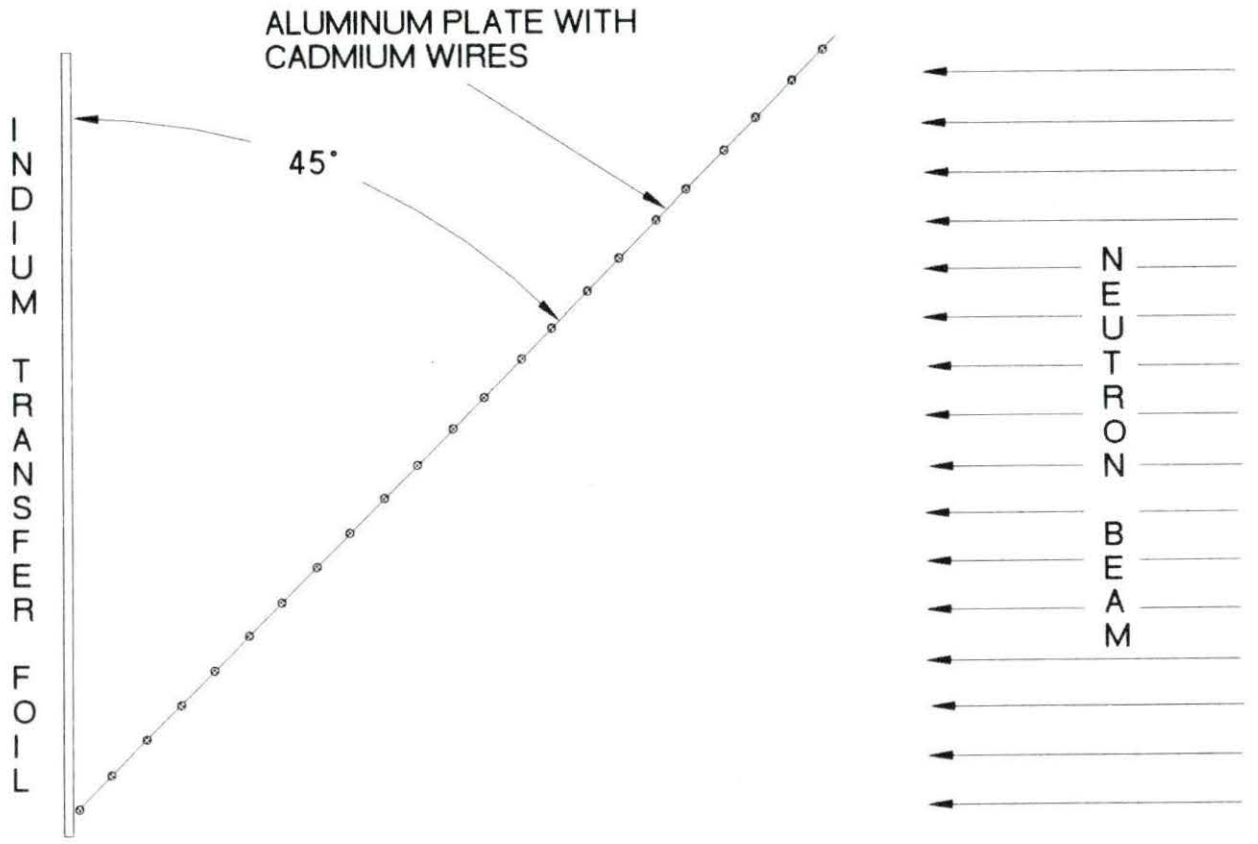

Figure 5.2: The Setup of The Transfer Foil and Cadmium Wires Used to Determine the L/D of the Facility

Figure 5.3: Neutron Radiograph of The L/D Apparatus

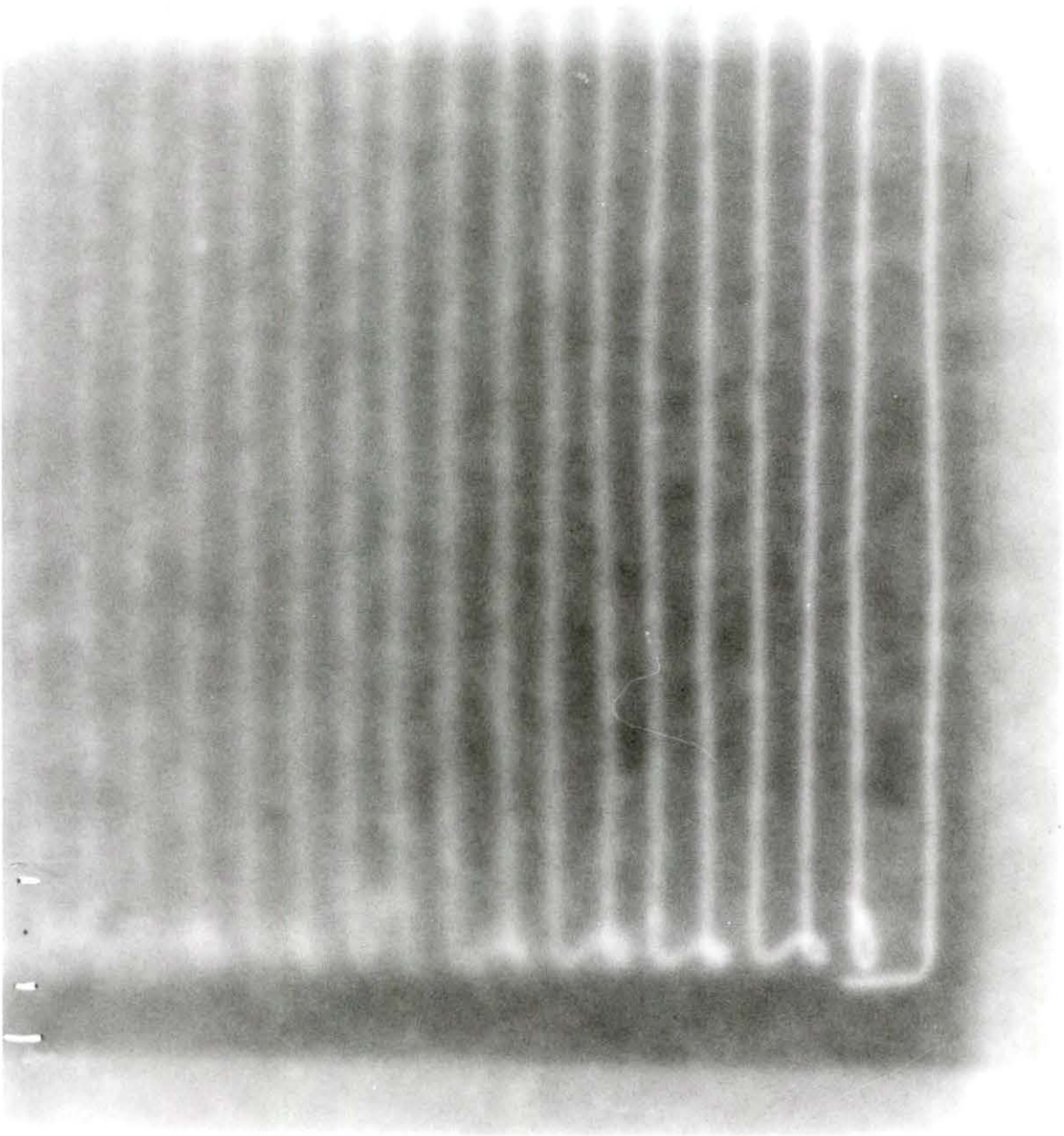

cadmium wire and the background film density that the "valley" was "riding." The resulting plot of film density vs position, Figure 5.4, was then examined to determine at what distance between the cadmium wire and indium transfer foil the umbra disappeared and the peak intensity decreased. This quantified inspection yielded the same value for L/D, at least 35 but not more than 42, as the visual inspection.

Beta Contribution to Film Density

The film density response of x-ray film depends on the type and energy of the radiation to which it is exposed. The indium foil used to transfer the image produces two types of radiation, beta and gamma rays, at many different energies. The beta radiation should be much more effective than the gamma radiation in exposing the film because the beta particle deposits more energy as it passes through the film. There are approximately two gamma rays and one beta particle emitted per disintegration of the indium-116m_1 isomer [37]. The yields and energies of the most probable gamma and beta particles are listed in Tables 5.1 and 5.2. To determine the effectiveness of each type of radiation, two radiographic images on x-ray films were produced from each transfer foil. One of the x-ray films was shielded from the beta rays emitted by the indium foil while the other x-ray film was exposed to both the gamma and beta rays.

The shielding of the beta rays was accomplished by using the aluminum support plate. The 2 mm thick aluminum plate used to support the indium was thick enough to shield the film from most of the beta particles produced by the decay of the indium-116m_1 isomer. The aluminum plate could stop beta particles with energies of up to 1 MeV. The same aluminum support plate still allowed the transmission of more than 99% of the gamma rays to the x-ray film.

The method used to determine the effectiveness of the two radiations at exposing the x-ray film assumed that the "toe" region of the "characteristic curve" of x-ray film density vs

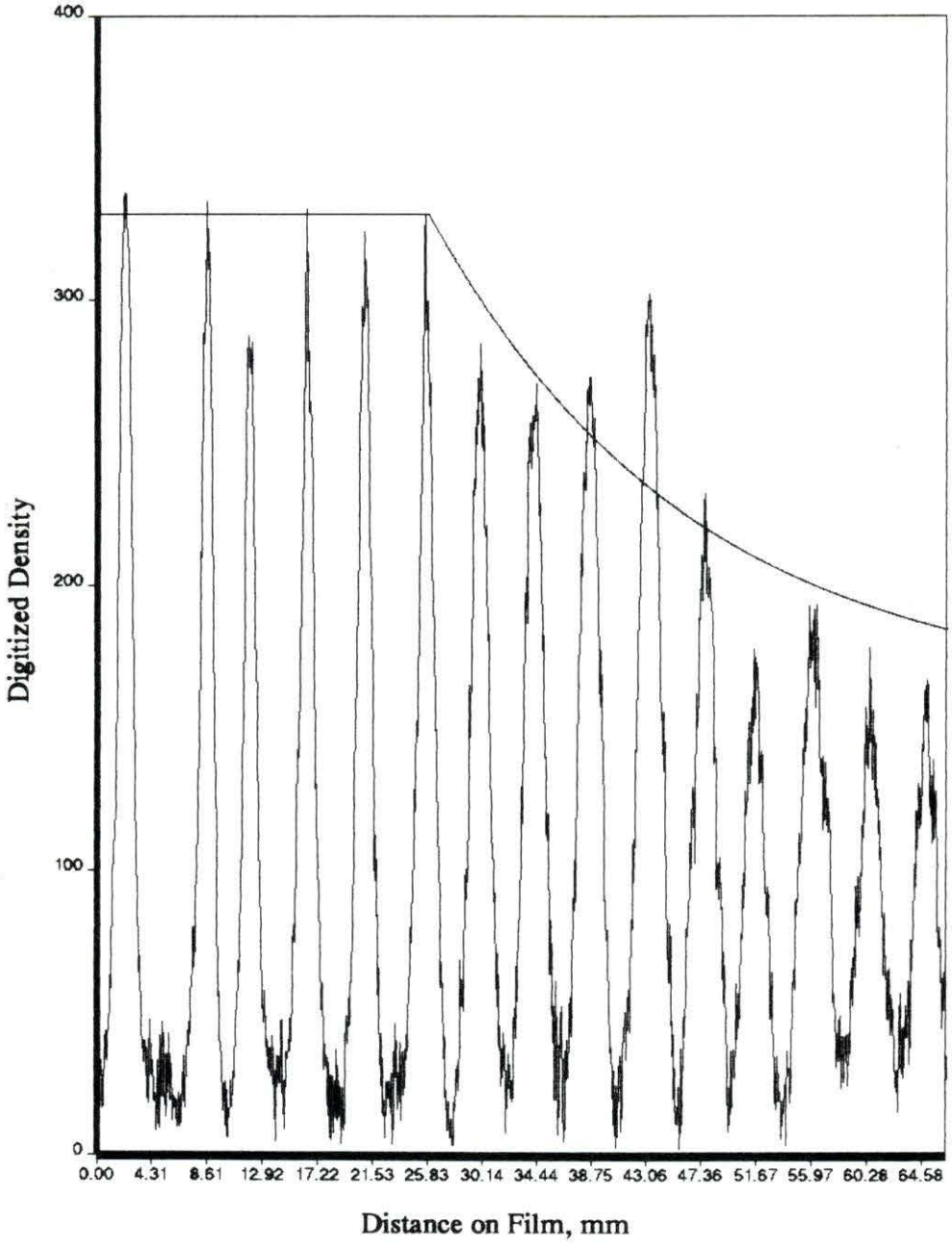

Figure 5.4: Film Density vs Position for L/D Determination

Table 5.1: Most Probable Gammas Produced From Decay of Indium-116m_1

Yield	Energy (MeV)
0.84500	1.2935
0.55348	1.0972
0.27801	0.4170
0.11577	0.8187
0.09887	1.5076

Table 5.2: Most Probable Betas Produced From Decay of Indium-116m_1

Yield	Maximum Energy (MeV)	Average Energy (MeV)
0.508	1.0094	0.351
0.328	0.8711	0.295
0.102	0.5991	0.190
0.027	0.3544	0.104

incident radiation dose was negligible, and that the curve was linear through out the range of film densities recorded. The "characteristic curve" of film density vs radiation exposure is shown in Figure 5.5.

The portion of the film density due to the beta particles was determined by comparing the film densities in the regions of the two films corresponding to the same location on the indium transfer foil. The film densities were measured with a densitometer, and the film fog densities were subtracted to remove any affects from unequal fog densities. These measurements were taken from four different sets of radiographs to ensure a good sample. All of the measurements from the radiographs gave similar results.

Using the procedure outlined, the beta particles were determined to contribute 85% of the film density. This value agrees with measurements made by health physicists, who found that 90% of the biological dose from the indium transfer foil was from beta particles.

This parameter was important as it determined the type of film cassette that could be used to hold the x-ray film during exposure from the transfer foil. The x-ray film could not be exposed to ambient room light, but the cassette should still allow exposure by as many beta and gamma rays as possible. The cassette used during exposure to the transfer foil was constructed from two layers of black construction paper with the edges sealed with electrical tape.

Epi-Cadmium Neutron Contribution to Film Density

The contribution to film density due to epi-cadmium neutrons was due to the combination of large epi-cadmium neutron absorption resonances in the isotope of indium used to transfer the image and a significant portion of the neutron flux in the epi-cadmium energy region. The absorption properties of any material examined depend on the energy of the neutrons used; generally, as the energy of the neutron increases, the differences in nuclear properties of the

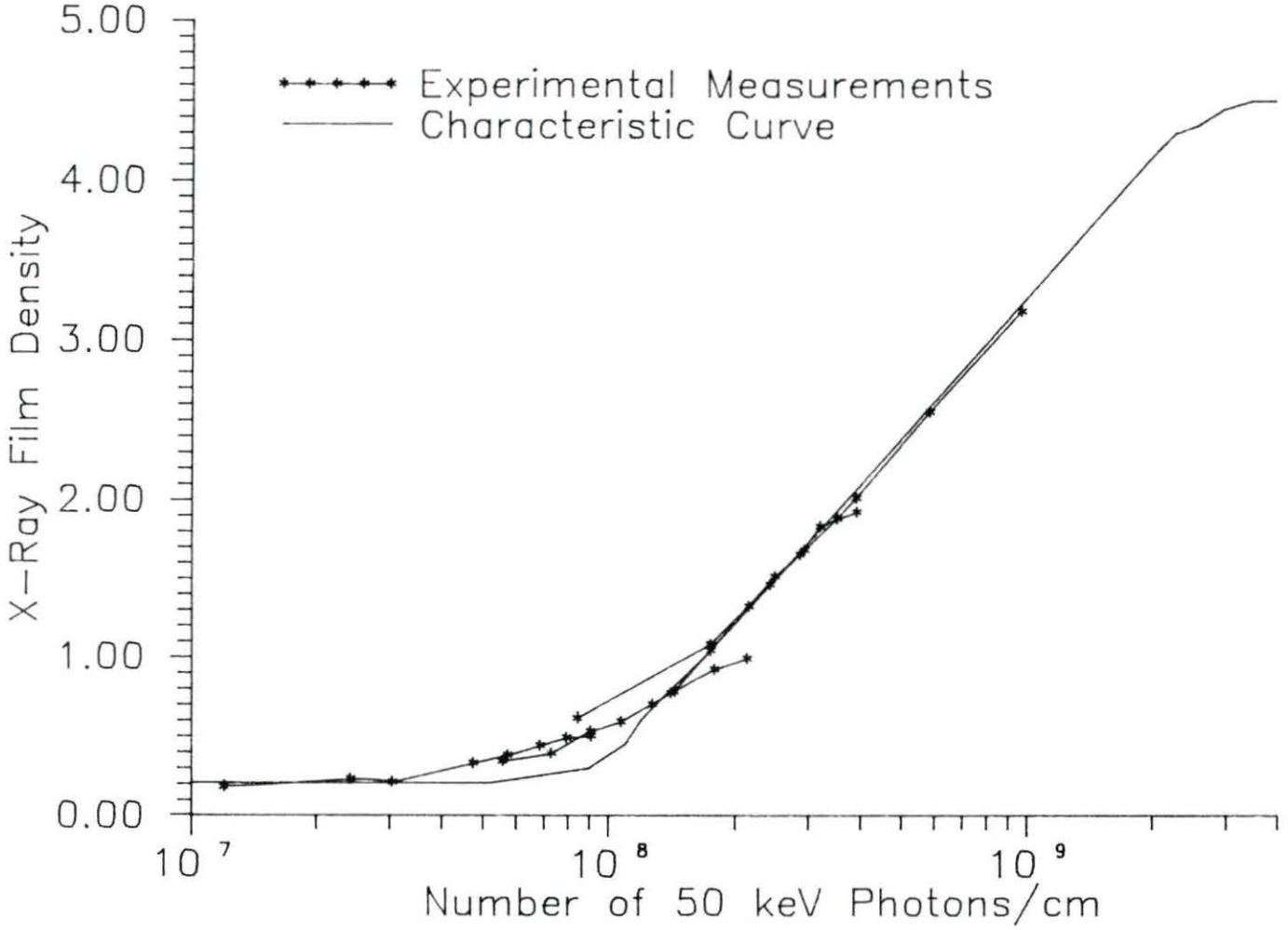

Figure 5.5: Characteristic Curve of X-Ray Film Density vs Radiation Exposure

different materials decrease. The epi-cadmium component of the film density then decreases the total possible contrast available by adding a constant background to the film.

To determine the epi-cadmium contribution to film density, the film densities of portions of radiographs corresponding to 40 mil thick cadmium disks were compared. The film density of the cadmium portions of the image were considered to be due to activation of the transfer foil by epi-cadmium neutrons. The background film densities elsewhere on the image were considered to be due to both thermal and epi-cadmium neutrons. The contribution to film density by the epi-cadmium neutrons was then just the epi-cadmium film density divided by the background film density. The calculations indicate that 30% of the image was due to epi-cadmium neutrons.

Scattered Neutron Contribution to Film Density

The contribution to film density from scattered neutrons would definitely be a material dependent property. Aluminum was the material used to examine this contribution to film density. As with the epi-cadmium contribution to film density, the scattered neutron contribution to film density decreases the total amount of contrast which could be used to highlight the desired aspects under investigation. Neutron scattering should dominate the neutron interactions in aluminum because the macroscopic scattering cross-section is 0.084/cm and the macroscopic absorption cross-section is only 0.015/cm [45]. The scattered neutron contribution to film density is assumed to be uniform over the image transferred by the indium foil.

The experiment used to determine the scattered contribution was similar to the procedure described in ASTM Standard E 545-86 [44]. The experiment used 40 mil thick cadmium disks affixed to either side of a 0.5 inch thick aluminum block. The experimental sample is shown in Figure 5.6. The neutron radiograph of the sample is shown in Figure 5.7. The film density on

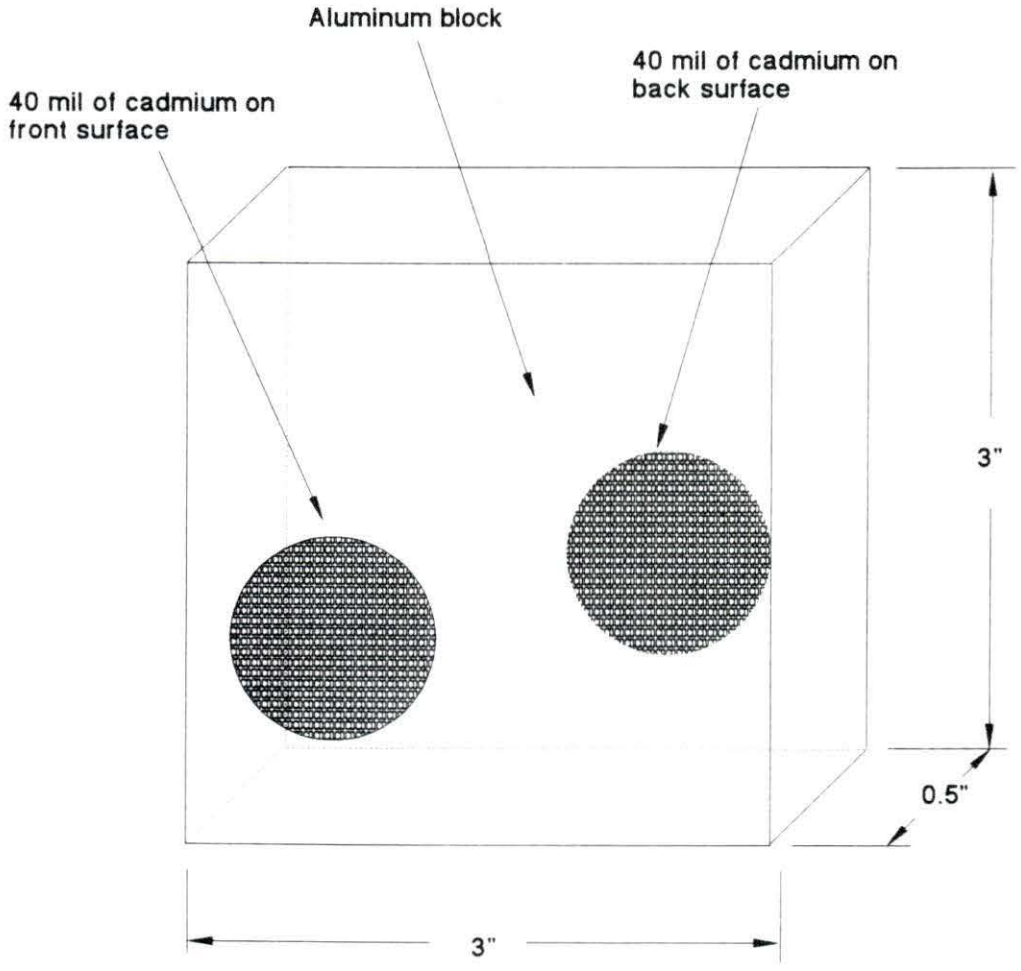

Figure 5.6: Aluminum Sample Used to Determine the Scattered Neutron Contribution to Image

Figure 5.7: Neutron Radiograph of The Aluminum Sample Used to Determine The Contribution of Scattered Neutrons to Film Density

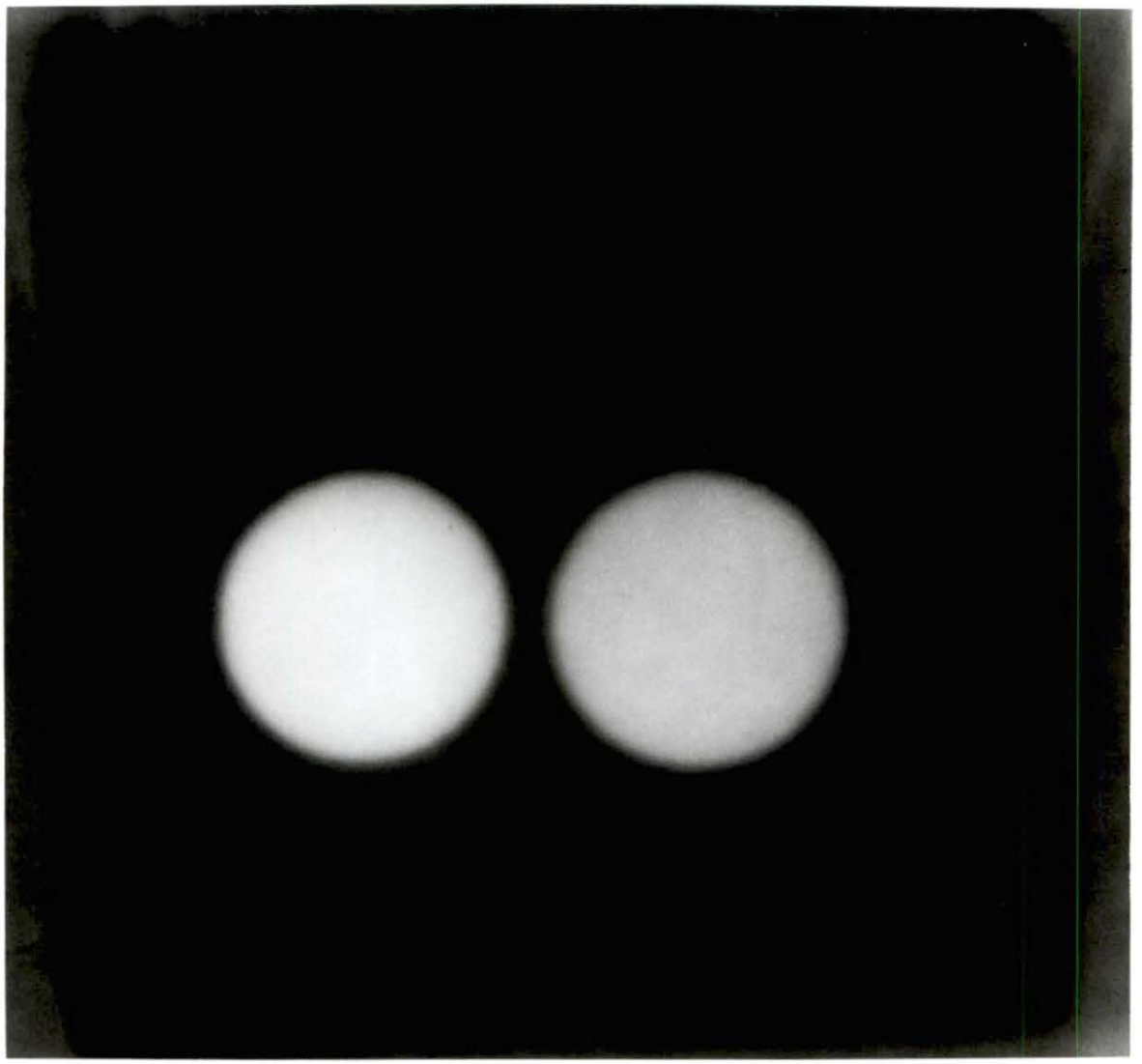

the radiograph, corresponding to the cadmium disk close to the indium transfer foil, gives only the epi-cadmium contribution to film density. The film density of the radiograph corresponding to the cadmium disk on the opposite side of the aluminum block gives the contribution from both the neutrons scattered by the aluminum and the epi-cadmium neutrons. The contribution of scattered neutrons in a 0.5 inch thick aluminum sample would then be given by the difference of the two film densities divided by the maximum background film density.

The data indicate that scattered neutrons account for approximately 7% of the film density for neutron radiographs of a 0.5 inch thickness of aluminum. The same thickness of metals such as iron or zirconium should give similar results, because the macroscopic scattering and absorption cross-sections are similar to those of aluminum; however, the best way to estimate how this parameter could affect an image is to compare the macroscopic absorption and scattering cross-sections of the materials radiographed. Also, a thicker sample would imply a greater number of scattered neutrons.

Film And Transfer Unsharpness

Besides geometric unsharpness, there is film unsharpness and the unsharpness associated with autoradiography. Film unsharpness manifested itself as the blurring of sharp boundaries due to the interactions between the primary and secondary radiations and the x-ray film. For one MeV gamma radiations, upwards of 80 grains would be made developable for each quantum absorbed [46] and beta particles should make even more grains developable since beta particles deposit more energy as they slow down. The magnitude of the film unsharpness for one MeV gamma radiation should be about 0.2 mm [46].

The transfer unsharpness (the unsharpness due to the autoradiography of the indium transfer foil) was another contribution to the blurring of sharp edges as each of the neutron "quanta"

recorded in the transfer foil became a "point" source at a finite distance from the x-ray film. An estimate of 1.5 mm for the transfer unsharpness was calculated by using geometry, the average penetration distance of the beta particles, and the film-foil separation distance. The affects of the geometric, film, and transfer unsharpness were similar, and the magnitude of the predicted unsharpness was on the order of 2 mm.

The method used to determine the unsharpness in the neutron radiographs was modeled on an empirical method in Halmshaw [46] which was hypothesized by Klasens for determining unsharpness in x-ray applications. The method for x-ray determination used a lead sheet to define a sharp edge for densimetric analysis. The film density vs position is plotted in Figure 5.8. After plotting the film density vs position, a line was defined by the two positions where the film density corresponded to D_{max} - 0.16*(D_{max}- D_{min}) and D_{min} + 0.16*(D_{max} - D_{min}). The unsharpness was then defined as the distance along the film where the previously defined line intercepts the lines corresponding to the maximum and minimum film densities. The only difference between the two methods was the use of a 40 mil thick cadmium sheet to define a sharp edge. The radiograph was magnified and digitized to obtain a reasonable density distribution curve. The distance determined by the calculation was approximately 2 mm.

Unsharpness affects the ability of film to resolve small changes in contrast or small spatial separation. As an indication of how contrast aids in resolving closely spaced items, a 40 mil thick cadmium sheet with 42 mil diameter holes with separation distances as small as 8 mils was radiographed to determine how close the holes have to be before they cannot be resolved. The radiograph used for this determination is shown in Figure 5.9. This test of resolution indicated that all the holes could be resolved. The ability to resolve objects less than 0.2 mm apart contradicts the previous unsharpness measurement of 2 mm; but there was an enormous difference in the contrast of the two objects which allowed the holes to be resolved, even though they were less than 0.2 mm apart.

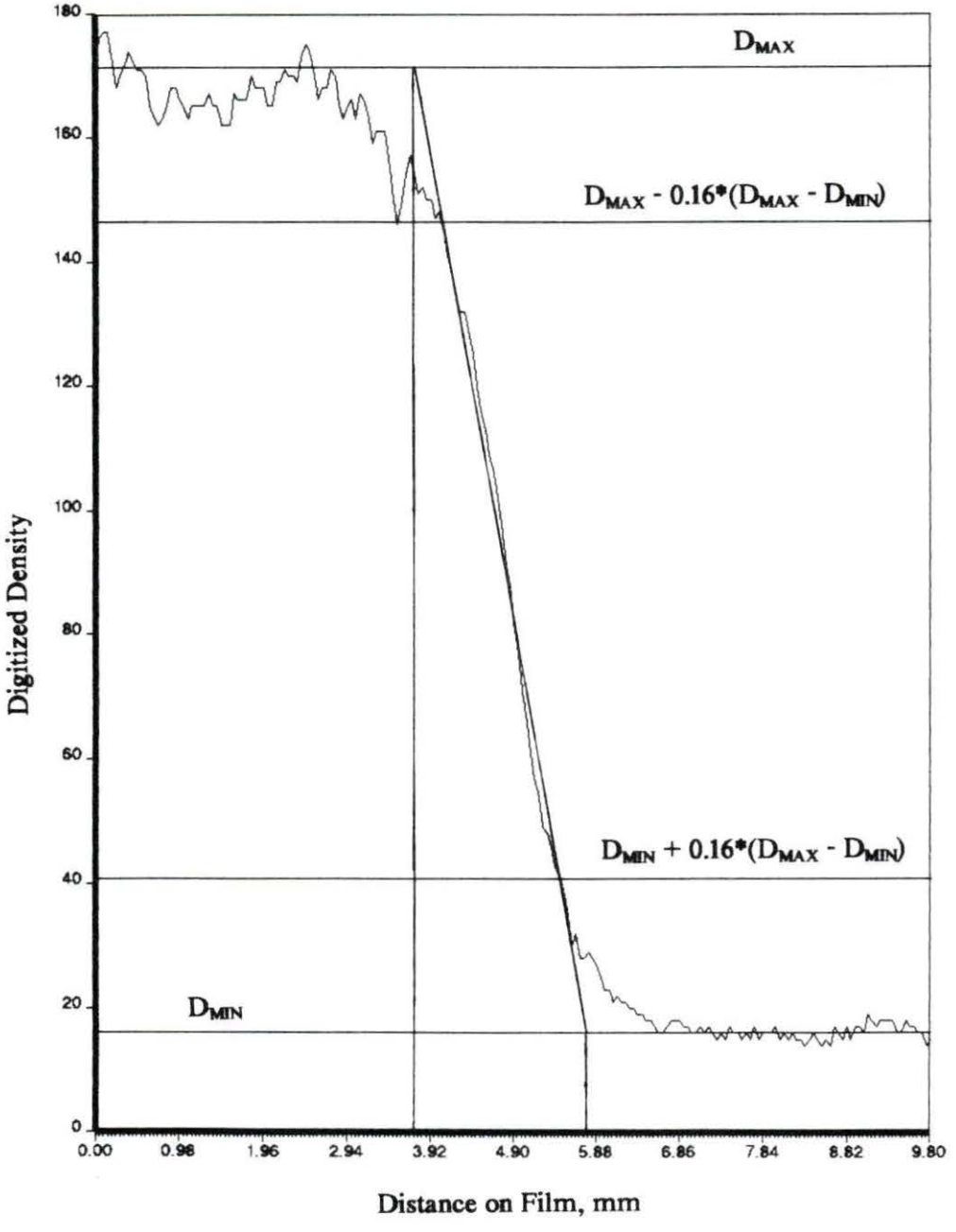

Figure 5.8: Film Density vs Position to Determine Unsharpness

Figure 5.9: Neutron Radiograph of Cadmium Plate With Small Diameter Holes to Measure Spatial Resolution

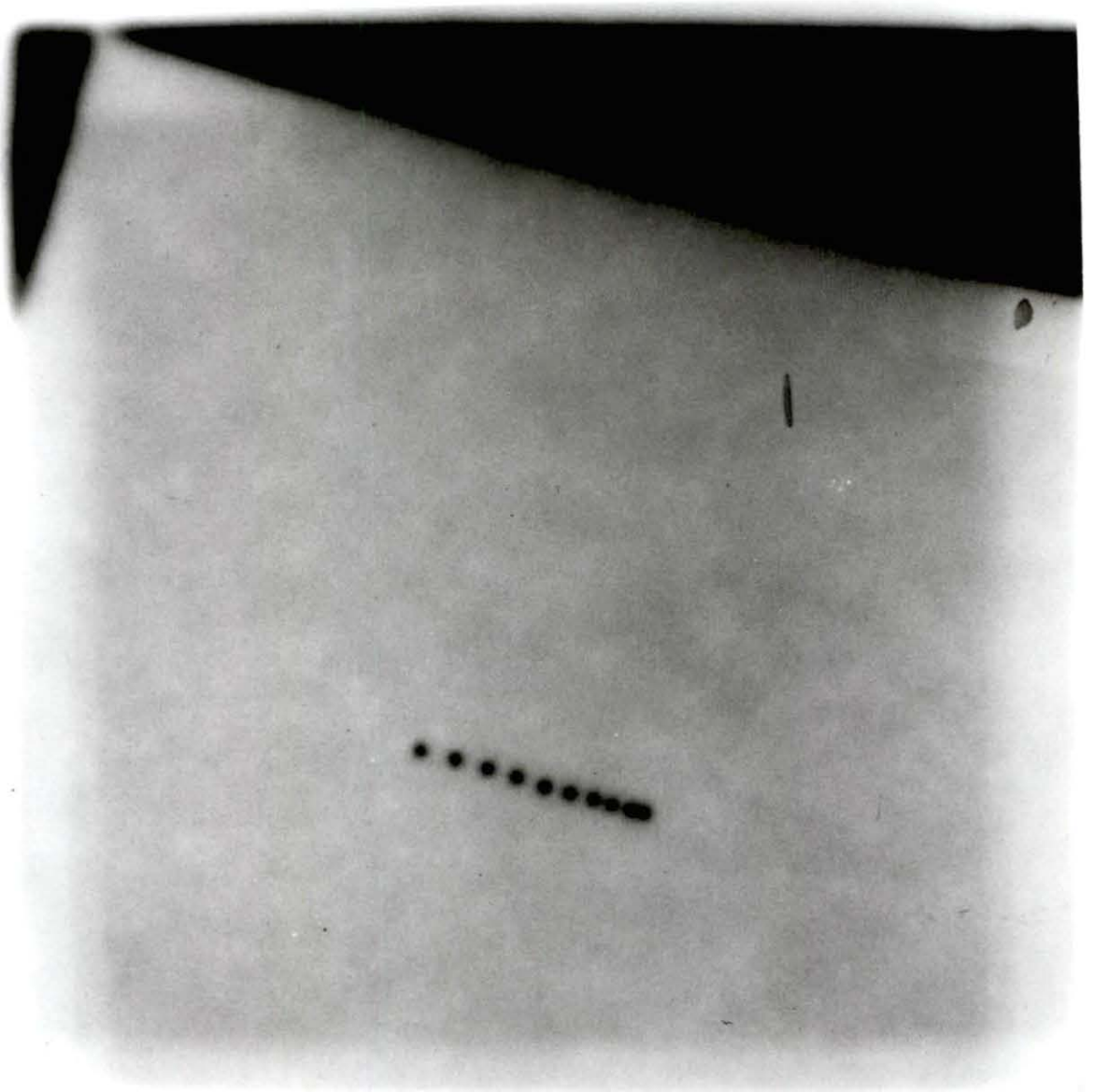

Film Mottling

Film mottling is the variation in film density which is not due to the object being radiographed. There are three possible causes of the mottling observed during neutron radiography; variations in the neutron beam, quantum mottling, and/or screen mottling due to variations in the transfer foil thickness or activity. Figure 5.10 shows a neutron radiograph of an aluminum block with aluminum hydroxide, $Al(OH)_3$, which is a material similar to the material present when aluminum has been corroded. There are three holes on the top of the block filled with this material which could be missed because the contrast between the holes and the material is close to the variation in the film density due to the mottling.

The first experiment performed with the NR facility was to determine the uniformity of the neutron flux across the beam and the actual neutron flux. Half-inch diameter foils of gold and indium were placed at two inch intervals across the beam in the vertical and horizontal planes. The values of the neutron flux determined from the foils fell within 2% of the average value. This indicates that the neutron flux was uniform and was not causing the mottling.

Quantum mottle is the result of statistical fluctuations in the spatial distribution of the radiations which expose the x-ray film. The amplitude of the fluctuations should vary as the square-root of the radiation fluence upon the image recording device. The radiation fluence that the film is subject to in NR was approximately $3x10^8$ decays/cm^2 from the indium foil, so the quantum mottle should only be 0.005%. The small value for quantum mottle eliminates it as the cause of the mottling.

To determine if the cause of the film mottling was due to the indium transfer foil, a new foil was rolled and used for a neutron radiograph in the hopes that the variation in film density would decrease with the new "smoother" transfer foil. Figure 5.11 shows the relative variation in

Figure 5.10: Neutron Radiograph of Aluminum Block With Simulated Corrosion

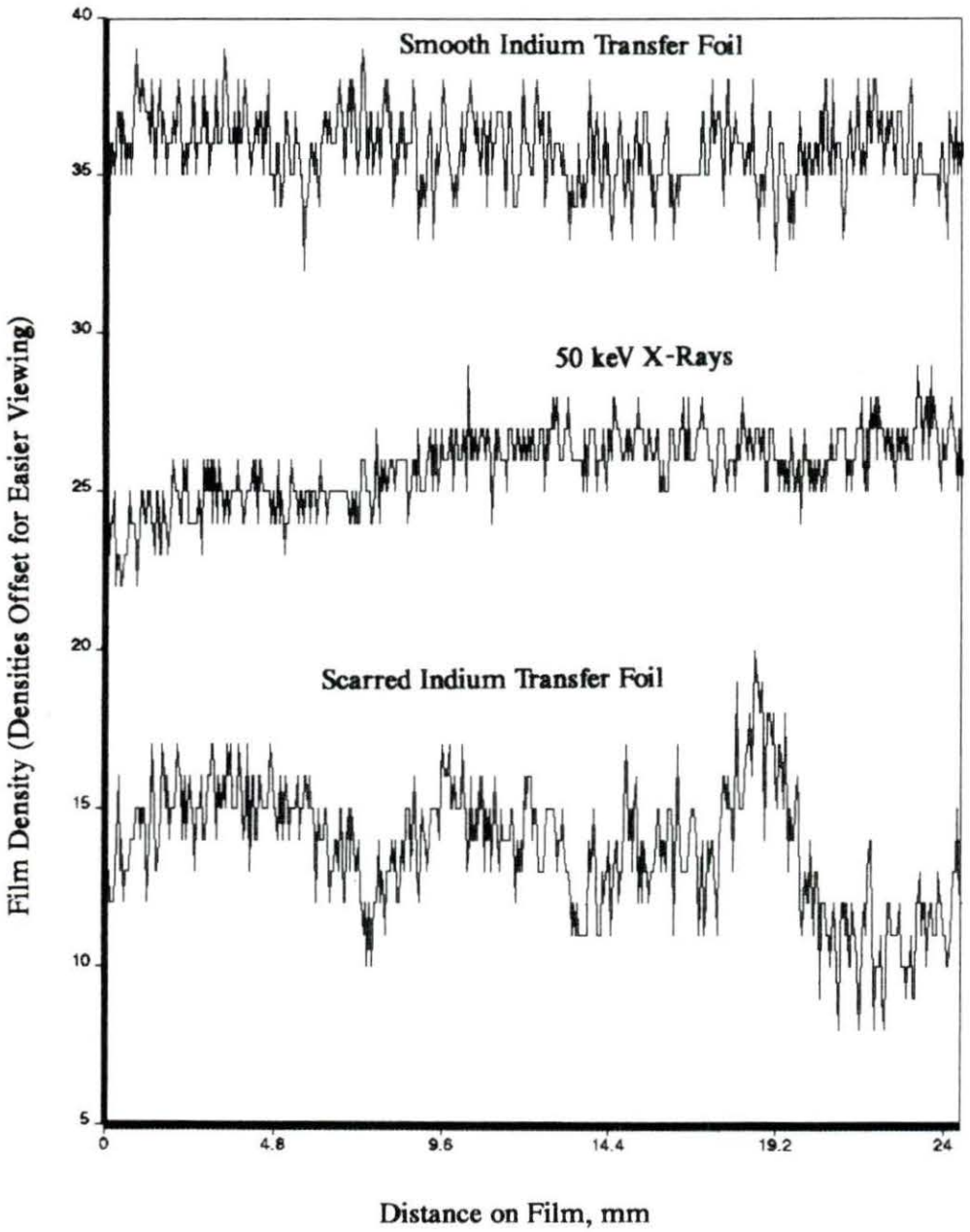

Figure 5.11: Small-Scale Density Variations for Smooth and Scarred Indium Transfer Foils and X-Rays on Kodak AA-1 X-Ray Film

film densities taken from digitized images. The film densities shown are from radiographs made from an older "scarred" indium transfer foil, a new "smooth" indium foil, and a 50 keV x-ray (50 keV maximum) image. The slices from smooth foil and the 50 keV x-rays appear to be less mottled than the one from the scarred foil indicating that much of the mottle was due to variations in the indium transfer foil.

CHAPTER 6. CONCLUSIONS

Measured Values of Important Parameters

The important parameters determined for the current NR facility are summarized in Table 6.1.

Table 6.1: Values of Parameters Affecting Neutron Radiography

Parameter	Measured Value
L/D	35
Thermal Neutron Flux	5.8×10^5 n/cm^2*sec
Cadmium Ratio	4.8
Beta Contribution to Film Density	85%
Gamma Contribution to Film Density	15%
Contrast Lost due to Epi-Cadmium Neutrons	30%
Contrast Lost due to Scattered Neutrons	7%
Total Effective Unsharpness	2 mm

The important aspects immediately evident from the parameters are: 1) the high contribution to film density by the beta radiation necessitates that the x-ray film packet have as little shielding as possible; and 2) there is a large loss in dynamic film range due to the epi-cadmium and scattered neutron contribution to the film density.

The total effective unsharpness is dominated by the unsharpness due to the indium transfer foil and the transfer of the image. This indicates that best avenues for improving the images in the future would be in increasing the cadmium ratio and minimizing the causes of the foil and transfer unsharpness. Increasing the cadmium ratio (decreasing the percentage of fast neutrons to the total number of neutrons) would increase the dynamic range available to contrast images on the x-ray film. Reducing the unsharpness would allow finer detail in the radiographic images to be resolved.

Comparisons With Temporary Facility

The temporary facility provided an opportunity to determine the feasibility of NR; but, other than a high neutron flux, it did not have good characteristics for NR. The characteristics of the temporary facility are compared with the new facility in Table 6.2.

Table 6.2: Comparison of the Two Facilities

Parameter	Temporary Facility Values	New Facility Values
L/D	16	35
Thermal Flux	$4x10^6$ n/cm^2*sec	$5.8x10^5$ n/cm^2*sec
Cadmium Ratio	4.2	4.8

To illustrate the difference between the characteristics of the two facilities, Figures 6.1 and 6.2 are radiographs from the temporary facility. Figure 6.1 is a radiograph of a BNC connector and an HN to BNC connector. Figure 6.2 is a radiograph of a butane lighter. Both of these

Figure 6.1: Neutron Radiograph of HN to BNC Connector Using The Temporary Facility

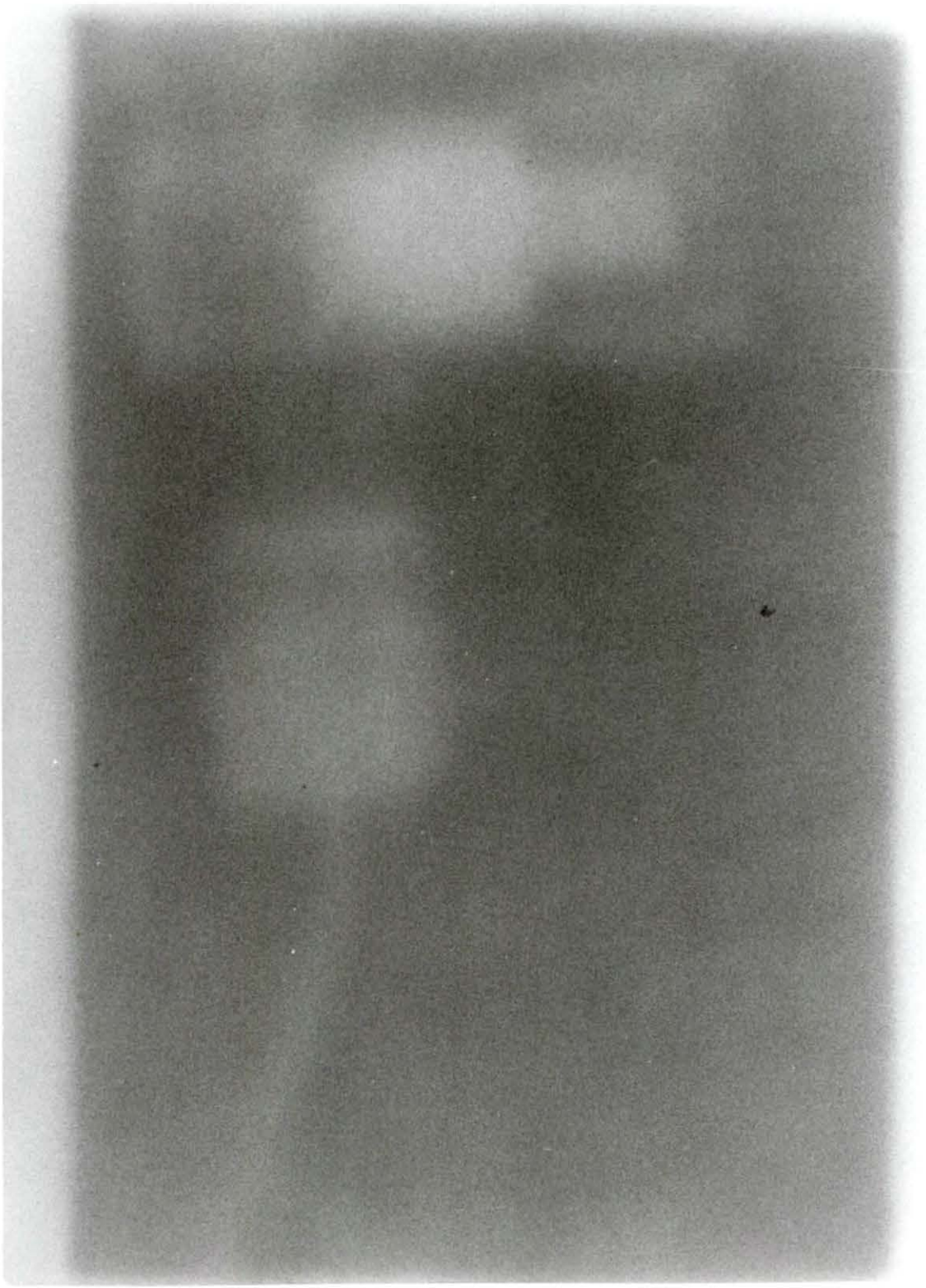

Figure 6.2: Neutron Radiograph of a Butane Lighter Using
The Temporary Facility

images show essentially blurry outlines of the radiography samples. Figure 6.3 is a radiograph of the same butane lighter and HN to BNC connector using the new facility. The internal detail of both radiography samples can be seen. The difference between the two facilities is readily visible.

Future Work

Increasing the cadmium ratio would increase the dynamic range on the film available to contrast radiographic images. This could be accomplished by using several mean-free paths worth of plexiglass to thermalize the fast neutrons. The current design for the collimator and source geometry would allow experimentation with an insert in the the center annular portion of collimator, and still have the necessary neutron flux to produce radiographs. The experimental measure indicating a 30% loss of contrast due to epi-cadmium neutrons would justify an attempt to reduce the epi-cadmium neutron flux.

The foil unsharpness could be reduced by using an indium foil of more uniform thickness. The foil could also be used to determine the foil's contribution to the unsharpness. Also, to decrease the unsharpness due to transferring the image, a film packet could be developed which would allow the foil and film to be in closer physical contact than the current arrangement.

The effective collimation of a source may depend on its shape. To examine this possibility the L/D of square and round source shapes could be investigated. It has been hinted that the use of a square source can triple the effective collimation for the same source area.

Work could also be done investigating the effects that different forms and energies of radiations have on film. The large yield in developable grains from high energy gamma and beta rays were not apparent. The number of 50 keV (50 keV maximum) x-rays necessary to

Figure 6.3: Neutron Radiograph of a Butane Lighter and an HN to BNC Connector Using The New Facility

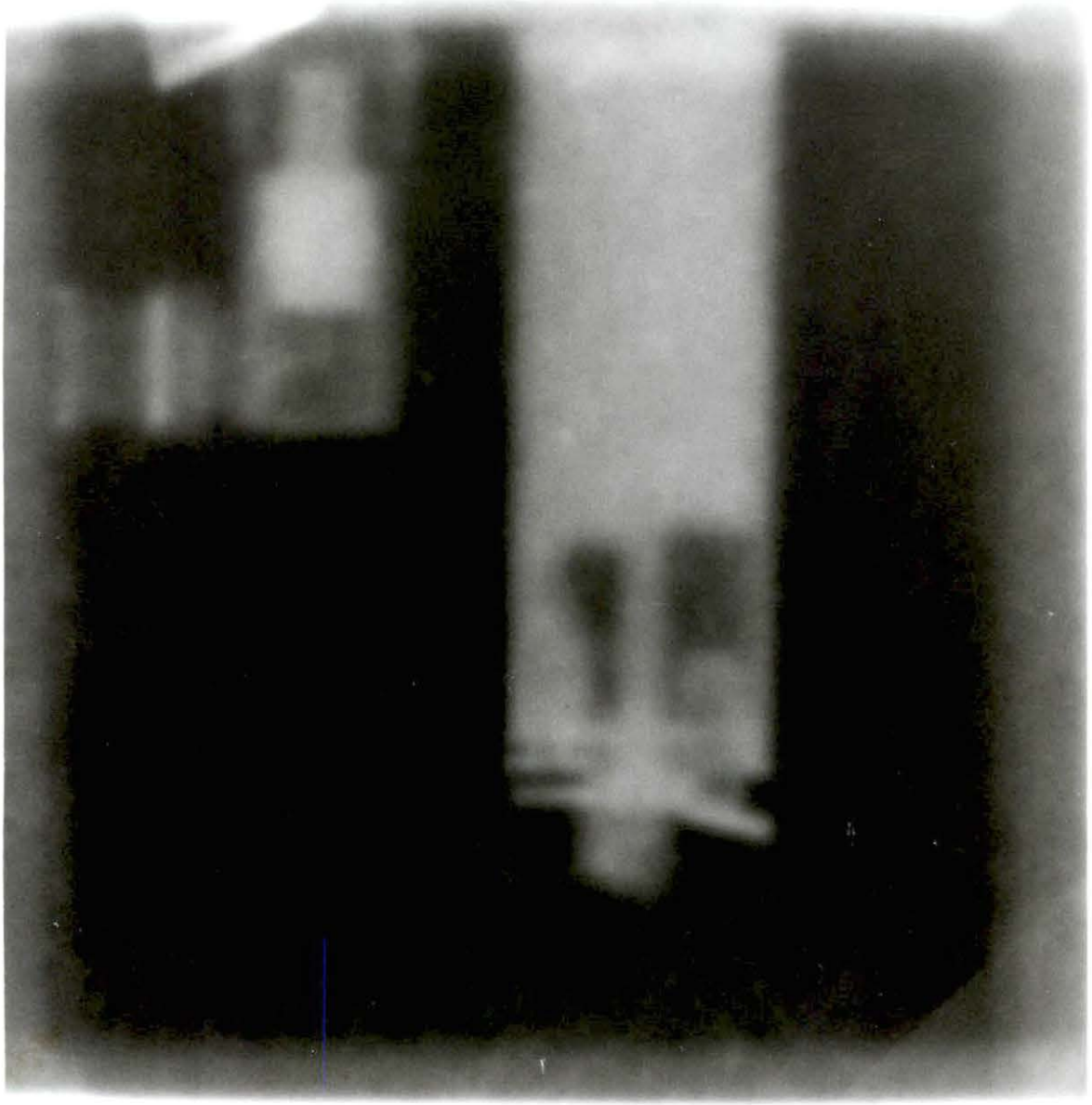

produce a given film density was of the same order of magnitude as the number of indium-116m_1 isomer decays to which the film was exposed. The claims of Halmshaw [46] and Herz [47] that higher energy gamma and beta rays could make 80 or more grains developable per radiation interaction does not appear to be substantiated.

BIBLIOGRAPHY

[1] W. C. Roentgen. "On a New Kind of Rays." *Nature*, 53, 274 (1896).

[2] H. Kallman and E. Kuhn. "Neutron Radiography." *Research Applied in Industry*, 1, 254 (1948).

[3] J. Chadwick. "Possible Existence of a Neutron." *Nature*, 129, 312 (1932).

[4] J. Thewlis. "Neutron Radiography." *British Journal of Applied Physics*, 7, 354 (1956).

[5] H. Rottger and P. Von Der Hardt. Neutron Radiography Handbook. Boston: D. Riedel Publishing Company, 1981.

[6] B. Harold. Neutron Radiography Methods, Capabilities and Applications. New York: Elsevier Publishing Company, 1965.

[7] J. P. Barton. "Neutron Radiography--An Overview." In Practical Applications of Neutron Radiography and Gaging. ASTM STP 586 (1976): 5-19.

[8] W. Schulz. "In Pool Neutron Radiography of BWR Control Rods Within The Scope of a Routine Refuelling Operation." In Proceedings of The Second World Conference on Neutron Radiography. Paris, France. (1986): 359-366.

[9] W. J. Oosterkamp and F.J. v.d. Kaa. "In Pool Neutron Radiography of a BWR Control Blade." In Proceedings of The First World Conference on Neutron Radiography. San Diego, Calif. (1981): 447-459.

[10] U. Bergenlid and I. Gustafsson. "Examination of Fuel Rods by Means of Neutron Radiography." In Proceedings of The First World Conference on Neutron Radiography. San Diego, Calif. (1981): 349-353.

[11] A.M. Ross. "Detecting Cladding Leaks in Irradiated Fuel Elements by Neutron Radiography." In Practical Applications of Neutron Radiography and Gaging. ASTM Special Technical Publication 586 (1976): 195-209.

[12] K.D. Kok. "Neutron Radiography of Nuclear Fuels at the Battelle Research Reactor." In Practical Applications of Neutron Radiography and Gaging. ASTM STP 586 (1976): 83-194.

[13] J. E. Lynn and D. K. Hyer, Editors. *Neutron Resonance Radiography.* National Technical Information Service, U.S. Department of Commerce, Springfield, VA, 1988.

[14] A. Tsurano. "Inspection of Pu Particle in UO_2-PuO_2 Pellet by Neutron Radiography." In Proceedings of The First World Conference on Neutron Radiography, San Diego, Calif. (1981): 365-373.

[15] C. N. Jackson, Jr., H. G. Powers, and C. A. Burgess. "Neutron Radiography of Fuel Pins." In Practical Applications of Neutron Radiography and Gaging. ASTM Special Technical Publication 586 (1976): 210-234.

[16] K. G. Golliher. "Neutron Radiography of Apollo Ordinance." In Proceedings of The First World Conference on Neutron Radiography, San Diego, Calif. (1981): 325-332.

[17] P. E. Underhill and R. L. Nawacheck. "Miscellaneous Applications of Neutron Radiography." In Practical Applications of Neutron Radiography and Gaging. ASTM Special Technical Publication 586 (1976): 252-267.

[18] P. L. Johnson. "Neutron Radiography as an 'In-Line' Product Acceptance Tool." In Practical Applications of Neutron Radiography and Gaging. ASTM STP 586 (1976): 125-133.

[19] J. P. Cassidy. "Use of a Low-Energy Van de Graaff Accelerator in Neutron Radiography of Encased Explosives." In Practical Applications of Neutron Radiography and Gaging. ASTM STP 586 (1976): 117-124.

[20] J. Joseph. "Californium Based Neutron Radiography for Corrosion Detection in Aircraft." In Practical Applications of Neutron Radiography and Gaging. ASTM STP 586 (1976): 168-180.

[21] J. J. Antal. "Experience With an On-Off Mobile Neutron Radiography System." In Proceedings of The Second World Conference on Neutron Radiography, Paris, France (1986): 407-414.

[22] V. Orphan, D. Kenden, and F. Johansen. "Mobile Neutron Radiography System for aircraft Inspection." In Proceedings of The Second World Conference on Neutron Radiography, Paris, France (1986): 447-454.

[23] J. Rant, R. Ilic, G. Pregl, P. Leskovar, and B. Zindar. "The Sensitivity of Neutron Radiography for Detection of Aluminum Corrosion Products." In Proceedings of The Second World Conference on Neutron Radiography, Paris, France (1986): 455-462.

[24] A. Ridal. and N. E. Ryan. "Neutron Radiography of Aluminum Alloy Corrosion Damage." In Proceedings of The Second World Conference on Neutron Radiography, Paris, France (1986): 463-470.

[25] W. E. Dance. "Neutron Radiography Nondestructive Evaluation of Aerospace Structures." In Practical Applications of Neutron Radiography and Gaging. ASTM STP 586 (1976): 137-151.

[26] N. B. Edenborough. "Neutron Radiography to Detect Residual Core in Investment Cast Turbine Airfoils." In Practical Applications of Neutron Radiography and Gaging. ASTM STP 586 (1986): 152-157.

[27] D. A. Froom. "Economics of Neutron Radiography for Commercial Aviation." In Proceedings of The Second World Conference on Neutron Radiography, Paris, France (1986): 423-430.

[28] W. G. Vernetson. "Development of Neutron Radiography at The University of Florida Training Reactor." Presentation at the 1988 Annual Meeting of the National Organization of Test and Research and Training Reactors, New Port, Oregon, 1988.

[29] F. M. de Mealemeester. "Operation and Utilization of the Argonaut Type Low Flux Reactor." Paper presented at the IAEA Consultant's Meeting on the Technology and Use of Low Power Research Reactors. Beijing, Peoples Republic of China. 1985.

[30] P.A. Gillespie and T. Wall. "Neutron Radiography at Lucas Heights." In Proceedings of The First World Conference on Neutron Radiography, San Diego, Calif. (1981): 85-89.

[31] J. J. Veenama, D. Mesman, and H. P. Leeflang. "Neutron Radiography Experiences at The Low Flux Reactor." In Proceedings of The First World Conference on Neutron Radiography, San Diego, Calif. (1981): 127-133.

[32] Nondestructive Testing Handbook, Volume 3. American Society for Nondestructive Testing, Columbus, OH, 1985.

[33] M. R. Hawkesworth, Editor. Radiography with Neutrons. Thomas Telford Limited, London, 1975.

[34] D. C. Cutforth. "Neutron Sources for Radiography and Gaging." In Practical Applications of Neutron Radiography and Gaging. ASTM STP 586 (1976): 20-34.

[35] A. A. Harms and D. R. Wyman. Mathamatics and Physics of Neutron Radiography. D. Riedel Publishing Company, Boston, 1986.

[36] D. J. Hughes and R. B. Schwartz. Neutron Cross Sections. 2nd Ed. U.S. Government Printing Office, Washington, D.C., 1958.

[37] C. M. Lederer and V. S. Shirley. Table of Isotopes. 7th Ed. John Wiley and Sons, Inc., New York. 1978.

[38] Code of Federal Regulations, Title 10, Part 20. U.S. Government Printing Office, Washington, D.C., 1957

[39] N. M. Schaeffer. Reactor Shielding for Nuclear Engineers. USAEC Technical Information Center, Oak Ridge, Tenn., 1973.

[40] J. C. Domanus. Collimators for Thermal Neutron Radiography. D. Riedel Publishing Company, Boston, 1987.

[41] F. W. Walker, D. G. Miller, and F. Fiener. Nuclides and Isotopes. 14th Ed. General Electric , Calif., 1989.

[42] E. P. Blizard. Reactor Handbook, Vol.3, Part B Shielding. 2nd Ed. Interscience Publishers, New York, 1962.

[43] J. R. Lamarsh. Introduction to Nuclear Engineering. 2nd Ed. Addison-Wesley Publishing Company, Menlo Park, Calif., 1983.

[44] 1987 Annual Book of ASTM Standards. Vol. 03.03. ASTM, Philadelphia, PA. 1987.

[45] J. J. Duderstadt and L. J. Hamilton. Nuclear Reactor Analysis. John Wiley and Sons, Inc., New York, 1976.

[46] R. Halmshaw. Physics of Industrial Radiology. Elsevier Publishing Company Inc., New York, 1966.

[47] R.H. Herz. The Photographic Action of Ionizing Radiations. John Wiley and Sons, Inc., New York, 1969.

APPENDIX A. MATERIAL EXPENDITURES

The following table lists the materials and costs incurred for the neutron radiography facility.

Table A.1: Purchases for Neutron Radiography

Item/Function	Cost ($ 1989)
Collimator	
Materials and Labor	943.41
Beamstop	
Boric Acid	116.16
Paraffin	225.60
Wood and Glue	30.00
Beamstop Total	371.76
Concrete Shielding	
Large Blocks	1255.00
Small Blocks	345.36
Concrete Total	1300.36
Overall Total	2615.53

APPENDIX B. RADIATION SURVEY OF SHIELDING

The real test of the shielding design was the radiation surveys which determined whether it was safe to use. The surveys were compiled by Tom Zimmerman on May 10 and May 15 of 1990 while the shield was used for neutron radiography. The survey of 1) gamma, 2) beta + gamma, 3) thermal neutron and 4) fast neutron doses is given in Table B.1. The locations which correspond to the measured doses are displayed in Figure B.1.

Table B.1: Doses Measured While Using Shield at Full Power

Location	Thermal Neutrons mR/hr	Fast Neutrons mrem/hr	Beta + Gamma mrem/hr	Gamma mR/hr
1	1.2	9	10	10
2	0.4	9	12	12
3	1.7	32	30	30
4	1.0	7	1.3	1.1
5	< 0.1	0.8	1.8	1.8
6	< 0.1	0.3	< 0.2	3.3
7	1.2	12	1.2	1.2
8	< 0.1	< 0.3	< 0.2	< 0.2
9	< 0.1	0.3	2.2	2.1
10	0.1	0.8	35	35
11	0.2	0.8	43	43
12	< 0.1	0.3	5	5
13	< 0.1	< 0.3	0.4	0.5
14	< 0.1	< 0.3	3	3
15	< 0.1	0.3	0.6	0.6
16	< 0.1	< 0.3	0.7	0.8
17	< 0.1	0.3	0.1	1.4
18	< 0.1	< 0.3	0.8	1.4

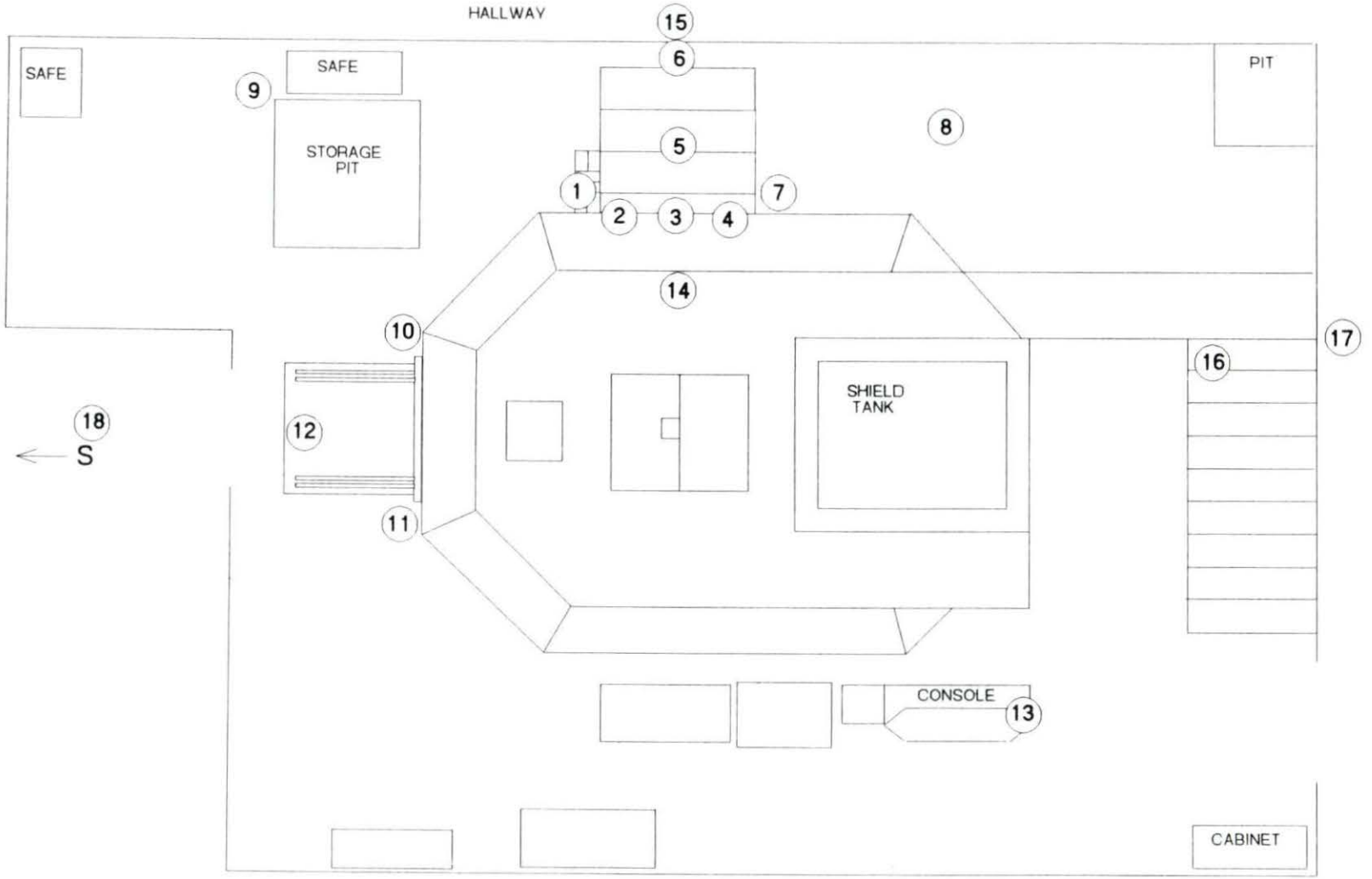

Figure B.1: Layout of Positions Where Doses Were Measured for the Shielding Survey

ACKNOWLEDGEMENTS

I would like to thank the CENTER for NDE and the Nuclear Engineering Department for allowing the use of equipment and time for the completion of my work and Power Affiliates for financial support. A special thanks is in order for Serhat Alten, Scott Carey, Dave Roth, and Dave Hamm for keeping the reactor running when I needed it and Tom Zimmerman for making sure I didn't fry myself pulling the hot indium transfer foils. Bob Williams also deserves my thanks for getting me involved in this project that has led into my thesis. Joe Gray and Dick Hendrickson will probably consider it thanks enough when they don't have to worry about my asking for advice, writing reports to the Reactor Use Committee, or proof-reading.

And finally, I would like to thank my mom and dad for supporting me through all my years of college and Jeannie for the past two years and the future years to come.